JASTIP
Japan - ASEAN
Science, Technology and
Innovation Platform

Annual Activity Report
on
Japan-ASEAN Science, Technology and Innovation Platform (JASTIP), Work Package 2 (WP2) – Energy and Environment

2018 Progress

TABLE OF CONTENTS

Annual Activity Report on Japan-ASEAN Science, Technology and Innovation Platform (JASTIP),
Work Package 2 (WP2) - Energy and Environment

P a g e 2 | 48

Innovations for Conversion of Biomass to High Value Chemicals by Photocatalytic Process

Annual Activity Report on Japan-ASEAN Science, Technology and Innovation Platform (JASTIP), Work Package 2 (WP2) - Energy and Environment

P a g e 3 | 48

1. Innovations for Conversion of Biomass to High Value Chemicals by Photocatalytic Process

Surawut Chuangchote[1], Navadol Laosiripojana[2], Verawat Champreda[3], Takashi Sagawa[4]

[1] Department of Tool and Materials Engineering, Faculty of Engineering, King Mongkut's University of Technology Thonburi (KMUTT), 126 Prachauthit Rd., Bangmod, Thungkru, Bangkok 10140, Thailand.
[2] The Joint Graduate School of Energy and Environment, Centre of Excellence on Energy Technology and Environment, King Mongkut's University of Technology Thonburi (KMUTT), 126 Prachauthit Rd., Bangmod, Thungkru, Bangkok 10140, Thailand.
[3] National Center for Genetic Engineering and Biotechnology, 113 Phahonyothin Rd., Klong Luang, Pathumthani 12120, Thailand.
[4] Graduate School of Energy Science, Kyoto University, Kyoto 606-8501, Japan.

Abstract

Application of photocatalytic processes for conversion of sugars which can be derived from lignocelluloses to energy and chemicals is considered a new promising environmentally friendly alternative which will play an important role in biorefinery and bioindustry related to valorization of sugars and agricultural wastes. This project aims to advance our technology on photocatalyst design based on the closed collaboration with Prof.Takashi Sagawa, Kyoto University under the JASTIP Renewable Energy program betweem NSTDA and Kyoto University (2015-2019). The project thmes will cover (1) continual research on fabrication and modification of photocatalysts for conversion of sugars to high-value chemicals (e.g. functional sugar derivatives) by improving the catalyst's specificity by fabrication techniques or surface modification and (2) design and assembly of a prototype photocatalytic reactor This concept on "photo-conversion on renewable biomaterials" will lead to the development of "photo-bio flow reactor" and will provide strong platform for conversion of sugars to value-added chemicals in integrative biorefinery.

Keyword   Biomass, Photocatalysis, Sugar conversion, Lignin utilization, High-value chemicals, Sugar derivatives

1.1   Introduction and Rational

Thailand is an agricultural-based country where lignocellulosic biomass can be considered as an important renewable energy resource for production of electricity, heat, liquid fuel, and commodity chemicals. This "biorefinery" concept can alleviate global warming due to the carbon neutral nature of the biomass and decrease the country's dependence of the depleting fossil resource. Biomass is the renewable resources (sustainable), which has its compositions similar to fossil fuel (contains C and H), and the products obtained from biomass are similar to those of petroleum. In details, lignocellulosic biomass is a multi-structure material. It consists mainly of three polymers i.e. cellulose, hemicelluloses, and lignin, which are associated with each other in

Annual Activity Report on Japan-ASEAN Science, Technology and Innovation Platform (JASTIP), Work Package 2 (WP2) - Energy and Environment

P a g e 4 | 48

addition to small amounts of acids, salts, and minerals. Currently several technologies, including catalytic, thermochemical, and biotechnological routes have been investigated for conversion of biopolymers-derived intermediates from various agricultural wastes to a spectrum of value-added products. However, these technologies are thermochemically and/or biochemically conversion processes which are limited by some restrictions in practice, such as high cost of reagents and equipment, high energy consumption, and harsh reaction conditions. Some processes have to use high chemical contents and more production steps for efficient biomass conversion into fuels and chemicals. These cause high capital investment in term of energy input and chemical usage. The exploration of new routes for the production of platform chemicals or fuels from biomass thus becomes increasingly important.

Photocatalysis is one of promising processes for energy and chemical productions, because it can be performed under solar irradiation at room temperature and mild condition. It offers the possibility of extending the spectrum of applications to a variety of processes, including oxidations and oxidative cleavages, reductions, isomerizations, substitutions, condensations, and polymerizations. In addition, it is considered as clean, effective, energy-saving, technology simple, ecologically benign, and low cost strategy. Photocatalysis is a well-established technique for many applications, e.g. wastewater or air treatment, pollutant degradation, and hydrogen (clean fuel) production by water splitting. Titanium dioxide (TiO_2) is the most important photocatalyst for many applications, such as degradation of organic pollutants (Hwang *et al.*, 2012), production of hydrogen (Gomathisankar *et al.*, 2013), self-cleaning surfaces (Murugan *et al.*, 2013), and dye sensitized solar cells (Cheng *et al.*, 2013). TiO_2 is a white solid inorganic substance that occurs naturally in several kinds of rock and mineral sands. It is a semiconducting material, which can be chemically activated by light with band-gap energy (Eg) of 3.2 eV. TiO_2 exists in 3 different crystalline modifications, i.e. anatase, brookite, and rutile, where anatase exhibits the highest overall photocatalytic activity (Park *et al.*, 2013). It is a popular catalyst to use in photocatalytic reactions, because TiO_2 has a highly oxidative, chemically stable, inexpensive, and nontoxic nature. TiO_2 nanoparticles have been prepared by different methods such as, chemical precipitation (Mashid *et al.,* 2006), chemical vapor deposition (CVD) (Shi, J., & Wang, X., 2011), sputtering (Song *et al.*, 2009), sol-gel technique (Bahadur *et al.*, 2011), hydrolysis, micro-emulsion method (Shen *et al.*, 2011), aerosol-assisted chemical vapor deposition (Tahir *et al.*, 2012), spray deposition (Bujnova *et al.*, 2010), thermal plasma (Tanaka *et al.*, 2011), hydrothermal method (Oh *et al.*, 2009), microwave-assisted hydrothermal synthesis (Melis *et al.*, 2012), solvothermal method (Zhang *et al.*, 2009), and the flame combustion method (Zhao *et al.*, 2007). Among these methods, sol-gel method is one of the most popular techniques for preparation of nanosized metal oxide materials with high photocatalytic activities (Su *et al.*, 2004; Tseng *et al.*, 2010).

In this proposed project, the application of photocatalytic approach for chemical production will be investigated based on the close collaboration between JGSEE, BIOTEC, and The University of Kyoto under the JASTIP Renewable Energy collaboration. The work will include the development of fabrication technology on synthesing highly efficient phototocatalysts and development of photocatalytic processes related to conversion of sugars and lignin to value-added chemicals. Together with the design and assembly of photocatlytic reactor with the concept on development of bio-energy devices in combination with efficient utilization of solar energy by Kyoto U., this collaboration will provide strong platform alternative technology for utilization of biomass in bio-industry which will contribute to the government's strategy on new S-curve industry.

1.2 Project Scopes

This project aims to develop high performance photocatalysts and photocatalytic reactor for production of target chemicals from glucose which can be obtained from 1st generation or 2nd generation raw materials in biorefinery. The project will focus on synthesis and fabrication of nano-scaled photocatalysts with improved performance and characterization of physicochemical properties of self-synthesized photocatalysts compared to commercial catalysts. The work will include the study of photocatalytic reactions on synthesis of high-value products (functional sugar derivatives) from glucose and application of the developed photocatalysts for production of target chemicals in photocatalytic reactor. The specific technical objectives are as follows:

(a)   To study the effects of fabrication conditions, doping and surface modification on morphotological appearances, physico-chemical properties, photocatalytic activity and selectivity of the photocatalysts

(b)   To study the effects of chemical structures of sugars on mechanisms of photocatalytic reactions

(c)   To study the reaction pathways for photocatalytic conversion of sugars (e.g. glucose) to its derivatives or unconventional sugars

(d)   To design and assemble a prototype laboratory-scale photocatalyic reactor (photo bio-flow reactor)

(f)   To study the reaction kinetics on sugar conversion to target chemicals in photo-bio flow reactor

1.3 Project Progress

1.3.1 Photocatalytic conversion of glucose to high value fuels and chemicals

TiO_2 photocatalyst was synthesized by combination of sol gel and microwave with different concentrations of a surfactant, called CTAB. The surface morphology of the photocatalyst was observed using a scanning electron microscope. It was found that the agglomeration of TiO_2 photocatalyst decreased with increasing concentration of CTAB **(Fig. 1)**. Therefore, the particle size of TiO_2 decreased with increasing concentration of CTAB. This is due to CTAB could reduce the surface tension and made high dispersion of TiO_2 precursor in the solution during the preparation process. In addition, CTAB could increase surface area of obtained catalysts, leading to high photocatalytic activity.
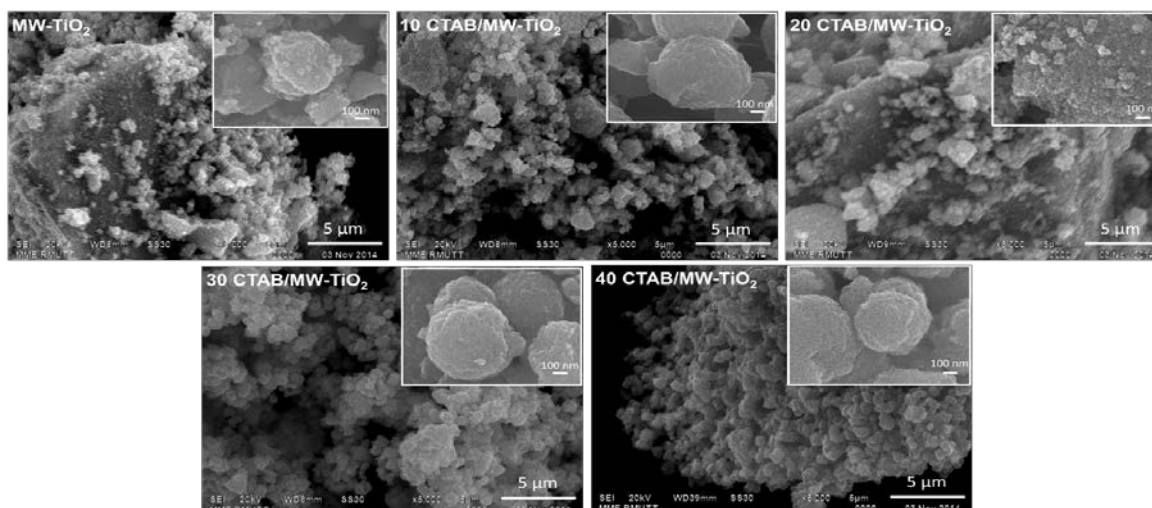
Fig. 1. SEM images of TiO$_2$ photocatalysts synthesized with different concentrations of CTAB.

The glucose conversions of various catalysts were carried out for 120 min under UV irradiation (wavelength = 365 nm). The results showed that high concentration of CTAB resulted in high glucose conversion. The highest glucose conversion of 60% represented in 40 CTAB/MW-TiO$_2$. It can conclude that high concentration of CTAB toward high surface area and low agglomeration of TiO$_2$, resulting in the highest glucose conversion **(Fig. 2)**. The product yields of glucose conversion are shown in Fig. 3. There are 4 products of glucose conversion; gluconic acid, arabinose, xylitol, and formic acid. It was observed that the yields of all products tended to increase with increasing irradiation time. The highest conversion of 60% after 120 min showed the yield of gluconic acid, arabinose, xylitol, and formic acid of 5%, 26%, 3% and 25%, respectively. From the yields of products, it indicated that use of CTAB tended to give high yields of arabinose **(Fig. 3)**.
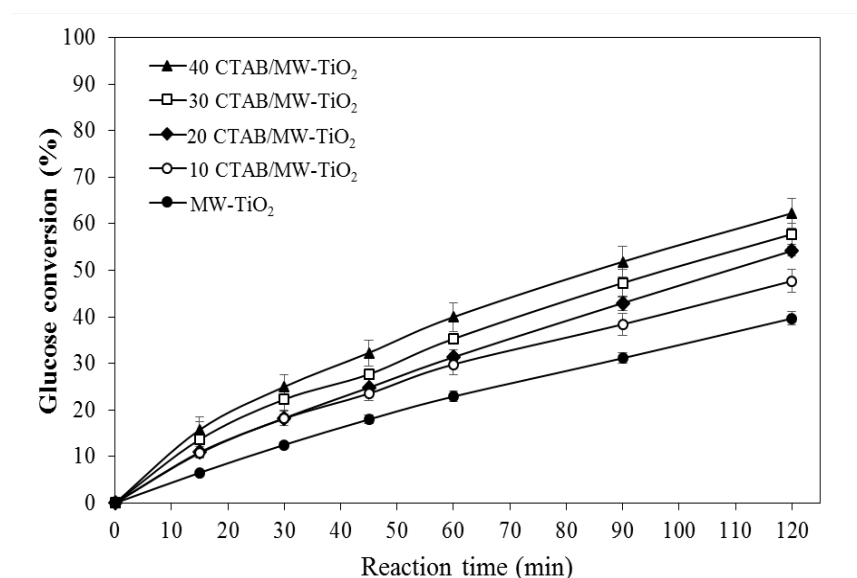
Fig. 2. Photocatalytic conversion of glucose with TiO$_2$ synthesized with different concentrations of CTAB in MW.
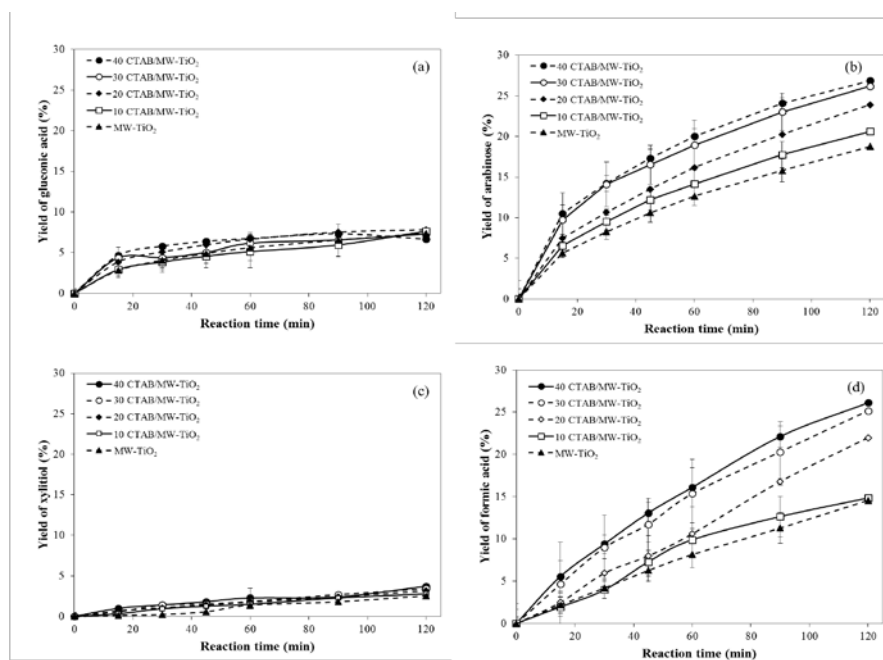
Fig. 3. Product yields of photocatalytic conversion of glucose with TiO_2 photocatalysts synthesized by different concentrations of CTAB.

As mentioned above, high surface area can enhance photocatalytic activity. So, the use of support materials is of interest for modification of TiO_2. The supports are expected to decrease agglomeration of TiO_2 and increase selectivity of photocatalytic reactions. From the group of supports, zeolites have been reported to delocalize band gap excited electrons of TiO_2 and thereby minimize electron-hole recombination to favor photoinduced electron-transfer reactions. SEM images show that surface morphology of zeolite changed after TiO_2 loading. It was found that the TiO_2 particles were coated on the surface **(Fig. 4)** compared with pristine zeolite. The TiO_2 coated on surface of zeolite showed well distribution. This caused the reduction of the agglomeration of TiO_2 nanoparticles synthesized with conventional process without zeolite. The catalyst size was increase when the amount of TiO_2 increased. Therefore, it was found that the specific surface area of TiO_2/ZeY increase compared with pure TiO_2.
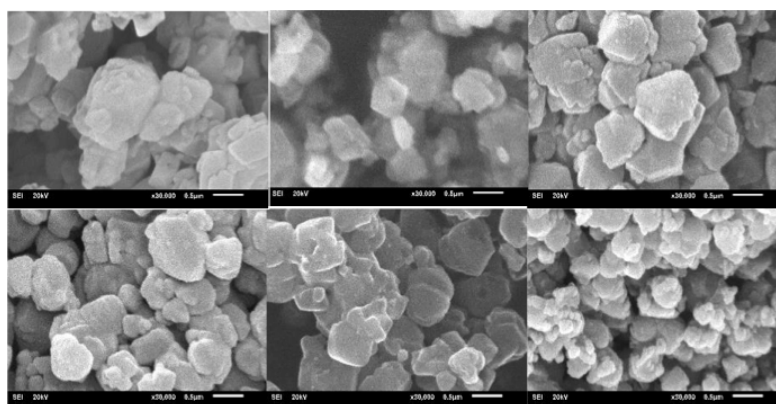
Fig. 4. SEM images (30000x) of ZeY, TiO_2(5%)/ZeY(95%), TiO_2(15%)/ZeY(85%), TiO_2(30%)/ZeY(70%), TiO_2(45%)/ZeY(55%), and TiO_2.

Annual Activity Report on Japan-ASEAN Science, Technology and Innovation Platform (JASTIP), Work Package 2 (WP2) - Energy and Environment

P a g e 8 | 48

The glucose conversion and organic compound yields increased with long irradiation time and reached a maximum value at 120 min. The results showed that zeolite supported TiO$_2$ (TiO$_2$/ZeY) represented higher photocatalytic conversion of glucose than pristine TiO$_2$ **(Fig. 5)**. However, it is distinct that the conversion rates did not increase linearly with increasing TiO$_2$ content. Certainly, the highest glucose conversion was achieved at a medium loading of 15% TiO$_2$ (75%) (Wang, C.C. *et al.* 2008). The yields of gluconic acid, arabinose, xylitol, and formic acid were 8.0, 29, 3, and 37%, respectively.
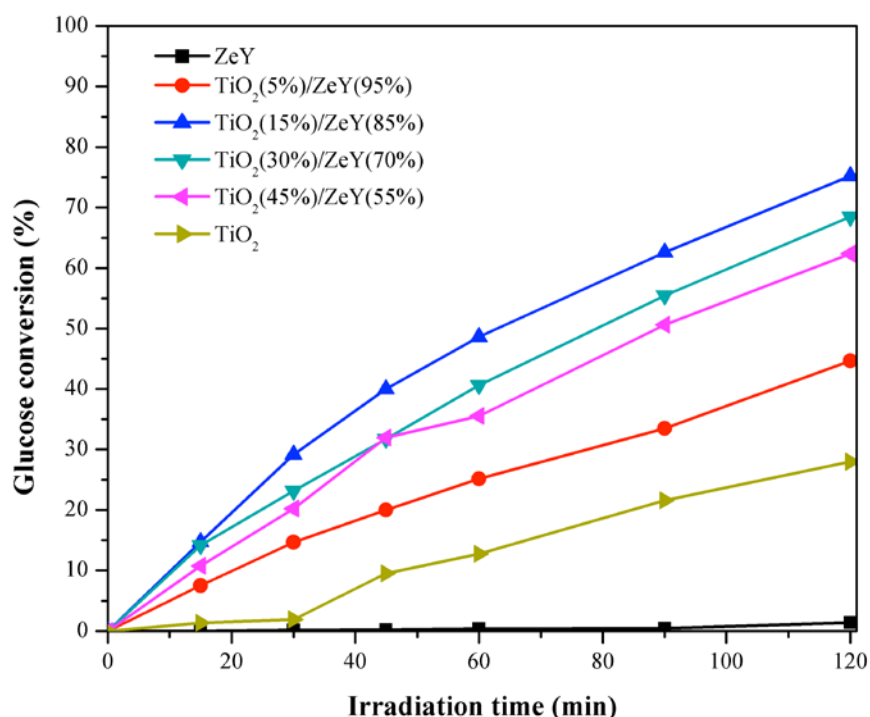
Fig. 5. Photocatalytic conversions of glucose under UV irradiation for 120 min with ZeY, TiO$_2$/ZeY (5, 15, 30, and 45 %wt), and TiO$_2$.

1.3.2 Modification of photocatalyst by non-metal doping

The presence of non-metal (B, C, and N) could be enhance glucose conversion compared with bare-TiO$_2$ as shown in **Figure 6**. The single doping of nitrogen on TiO$_2$ was achieve glucose conversion with 60%. In addition, modified TiO$_2$ with co-doping of boron and nitrogen showed the highest glucose conversion up to 90% for 180 min. The yield of gluconic acid, arabinose, xylitol, and formic acid were 9.0, 30.5, 8.9 and 47.6%, respectively.
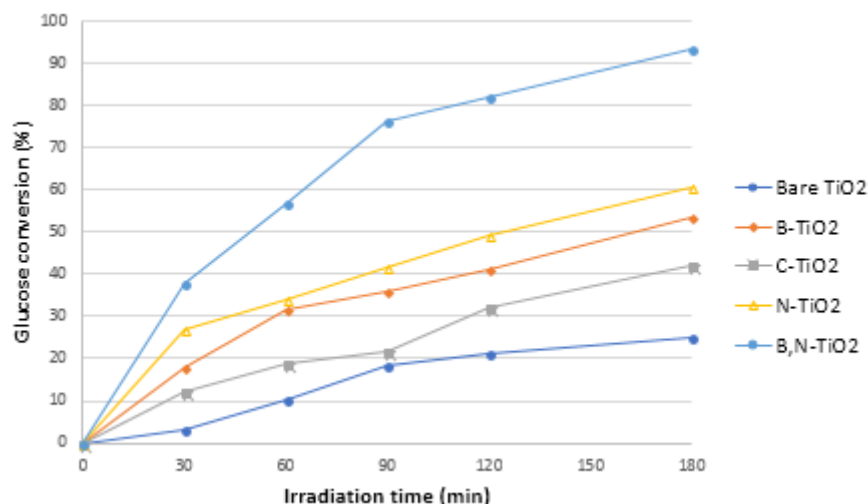
Fig. 6. Photocatalytic conversion of glucose under UV irradiation for 180 min in the presence of non-metal doping on TiO_2

The surface area of modified TiO_2 with non-metal is illustrated in **Table** 1. The increasing surface area was observed with the presence of C, B, N, and BN, respectively. This result was corresponded with the performance on glucose conversion. The presence of co-doping (BN) gave the highest surface area with 227.69 m^2/g. Thus, high surface area leading to improve the active site on photocatalyst resulted in enhancement of photocatalytic activity as the same report in previous part.

Table 1. The specific surface area of non-metal doped on TiO_2

Samples	Pore size (nm)	Pore volume (cm³/g)	Surface area (m²/g)
Bare TiO₂	5.55	0.11	77.92
B-doped TiO₂	3.99	0.15	147.37
C-doped TiO₂	4.37	0.12	109.20
N-doped TiO₂	5.47	0.21	153.04
BN-dopedTiO₂	5.56	0.32	227.69

In addition, the increasing of productivity and conversion also supported with the results of PL measurement as shown in **Figure 7 and 8.** It was found that doping of non-metal on TiO_2 resulted in decreasing the intensity on PL measurement because of the effective inhibited the recombination of electron and hole. Moreover, UV-vis reflectance showed slightly shift of absorption in the visible region. A wide absorption region led to increase the excited electron under irradiation resulted in high performance on glucose conversion

Annual Activity Report on Japan-ASEAN Science, Technology and Innovation Platform (JASTIP),
Work Package 2 (WP2) - Energy and Environment

P a g e 10 | 48
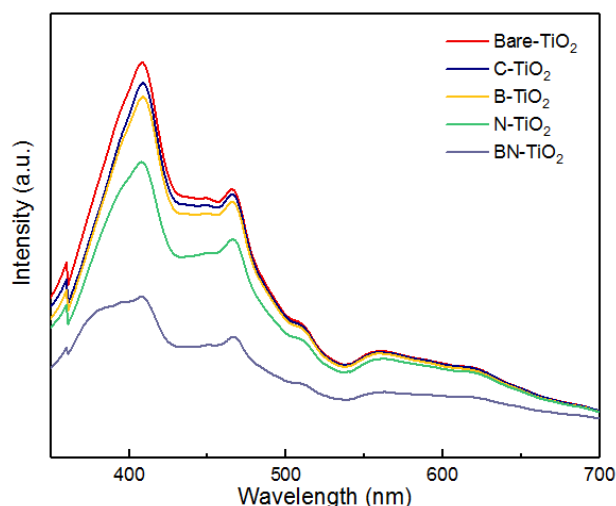
Fig. 7. Photoluminescence of non-metals doped TiO_2
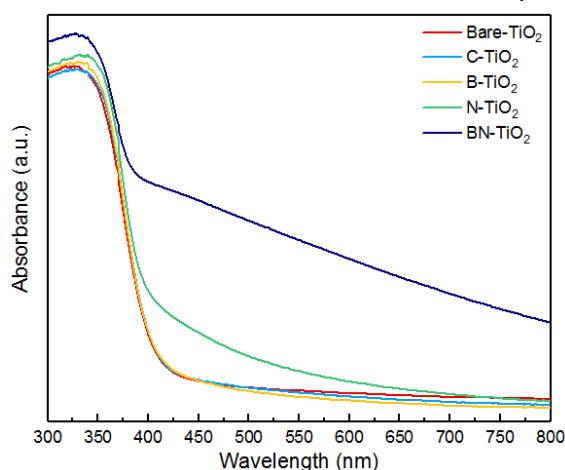
Fig. 8. UV-vis diffuse reflectance spectra of non-metal doped TiO_2

1.3.3 Photocatalytic conversion of glucose under visible light

In this study, the samples were irradiated under 450 W Xenon lamp equipped with sharp cut-off filter $\lambda > 380$ nm. The commercial of TiO_2 (P25) was used as benchmark as shown in **Figure 9**. The highest glucose conversion of P25 was observed at 9 h with 62%. The main product are formic acid and arabinose. Further, applied material as graphitic carbon nitride (g-C_3N_4) is a good candidate on photocatalytic conversion in term of productivity (**Figure 10**). The g-C_3N_4 could be enhance the conversion up to 77% at 12 h. Interestingly, the different main products of gluconic acid and formic acid were observed comparing with P25. The yield of gluconic acid, formic acid, arabinose, and xylitol were 35.2, 29.7, 8.9 and 4.4%, respectively.

Annual Activity Report on Japan-ASEAN Science, Technology and Innovation Platform (JASTIP), Work Package 2 (WP2) - Energy and Environment

P a g e 11 | 48
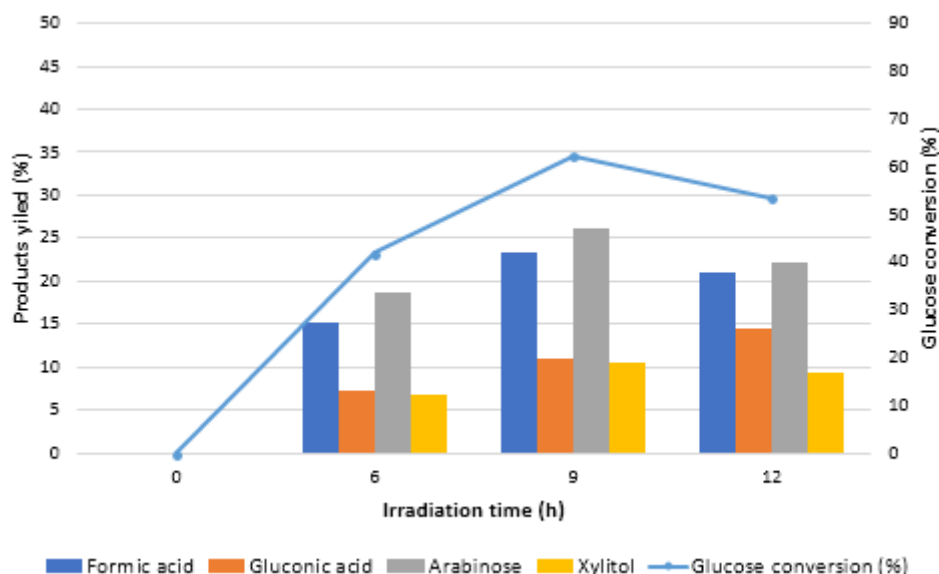
Fig.9. Photocatalytic conversion of glucose under visible light irradiation in the presence of TiO_2 (P25)
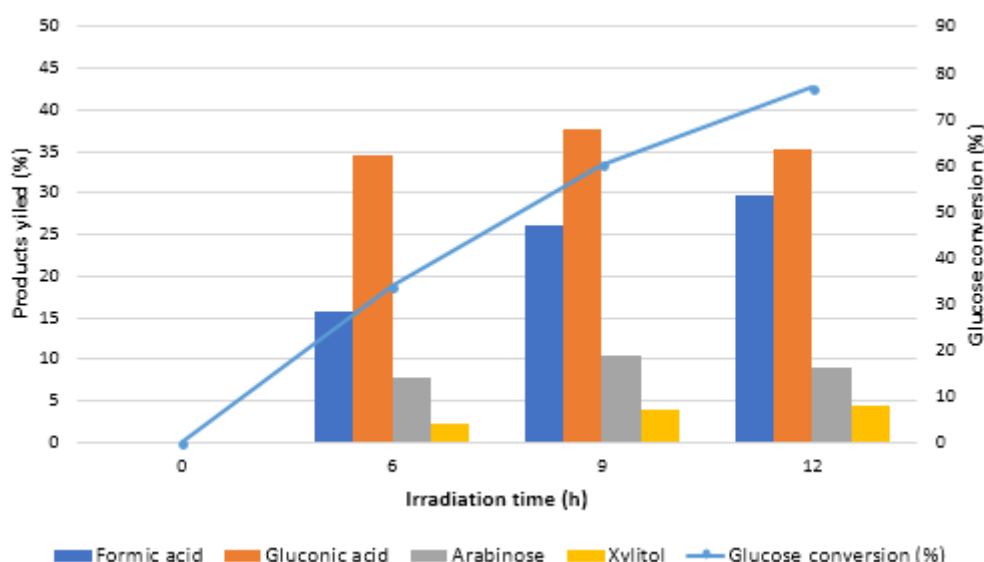
Fig.10. Photocatalytic conversion of glucose under visible light irradiation in the presence of graphitic carbon nitride (g-C_3N_4)

1.3.2 Photocatalytic conversion of lignin to high value fuels and chemicals

Cellulose is the main component of lignocellulosic, while lignin is the second abundant composition. So lignin has high potential for production of chemicals. There are many techniques to convert lignin to value added chemical, such as pyrolysis, gasification, and depolymerization. These technologies use high temperature and high energy consumption. So, photocatalytic is an interesting process. The photocatalytic conversion of kraft lignin catalyzed by P25 TiO_2 under UV irradiation present various products. The main products from lignin conversion are 2-methyl-napthalene, 4-hhydroxy-benzaldehyde, and vanillin **(Fig. 11)**.

Annual Activity Report on Japan-ASEAN Science, Technology and Innovation Platform (JASTIP), Work Package 2 (WP2) - Energy and Environment

P a g e 12 | 48
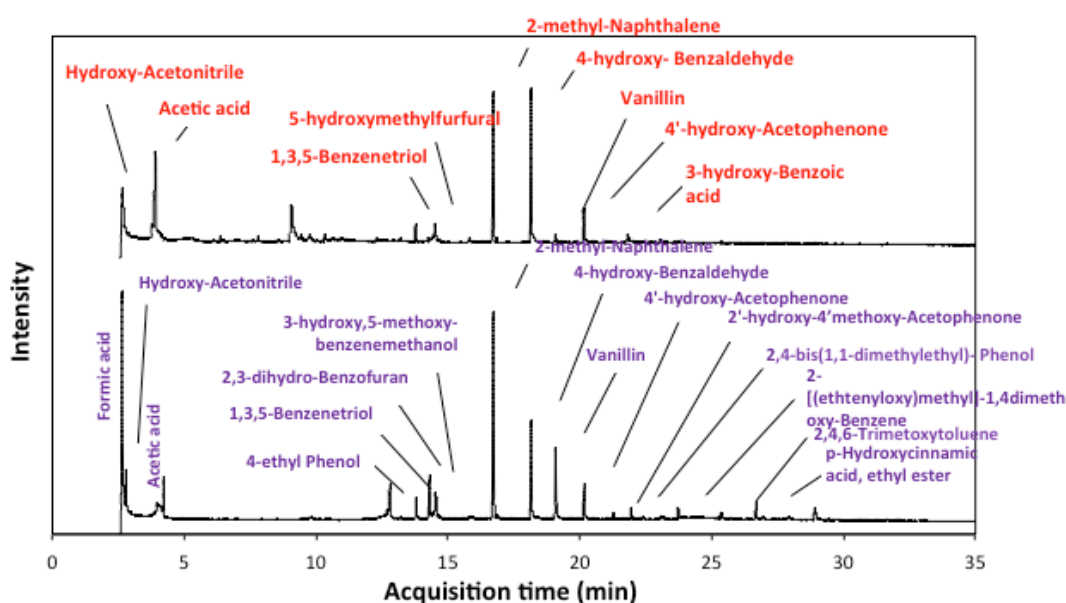
Fig.11. GC-MS spectra of hydrocarbon compounds derived from photocatalytic conversion of kraft lignin catalyzed by P25 TiO$_2$ under UV irradiation for 2 h and 5 h.

1.3.4 Combination of photocatalysis to conventional processes for enhancement of biomass pretreatment/hydrolysis

The pretreatment of biomass using photocatalytic process catalyzed P25 TiO$_2$ under UV irradiation for 24 h was preliminary carried out. The result showed that the amounts of individual sugar, as well as the total sugar yields, were low in the cases of no catalyst and no UV irradiation. TiO$_2$ photocatalysts could accelerate the separation of biomass compositions. Thus, a lot of products (native) were produced much compared with the photolysis **(Fig. 12)**.

	Bagasse + H2O	Bagasse + H2O + UV	Bagasse + H2O + TiO2	Bagasse + H2O + TiO2 + UV
Pentose(mg/g native)	47.00	50.09	45.12	49.07
Glucose(mg/g native)	59.60	67.46	60.88	78.18
Pentose (mg/g pretreated)	48.11	55.00	46.23	57.91
Glucose (mg/g pretreated)	65.18	89.36	71.09	75.71
Total sugar (mg/g pretreated)	93.53	131.22	97.27	119.49
Weight loss (%)	3.48	20.64	3.42	3.65
Catalyst in Solid Phase (%)	0.00	0.00	16.47	16.67

Annual Activity Report on Japan-ASEAN Science, Technology and Innovation Platform (JASTIP),
Work Package 2 (WP2) - Energy and Environment

P a g e 13 | 48

Fig. 12. Sugar digestibility yields in photocatalytic pretreatment (solvent = water) compared with blanks (no catalyst and/or no UV irradiation).

1.4 Conclusions

The photocatalytic reaction can convert glucose to value added chemical such as gluconic acid, arabinose, xylitol and formic acid. The modification of TiO_2 by CTAB and zeolite can improve the photocatalytic activity. TiO_2 can also be also used as photocatalyst to convert lignin to value-added chemicals. Some high value chemicals, e.g. 2-methyl-napthalene, 4-hhydroxy-benzaldehyde, and vanillin, were founded from the lignin conversion. Moreover, photocatalysis can be used for pretreatment of biomass. It was found that TiO_2 could accelerate the separation of biomass compositions better than photolysis.

1.5 Project Outputs

1.5.1 Publications (The publications in blue do not acknowledge JST as I mentioned to you before. Papers from number 7 has already cited JST.)

1. Navaporn Kaerkitcha, Surawut Chuangchote, and Takashi Sagawa (2016) "Control of physical properties of carbon nanofibers obtained from coaxial electrospinning of PMMA and PAN with adjustable inner/outer nozzle-ends," Nanoscale Research Letters, 11(1), 1-9.
2. Witchaya Arpavate, Surawut Chuangchote, Navadol Laosiripojana, Jatuphorn Wootthikanokkhan, and Takashi Sagawa (2016) "ZnO Nanorod Arrays Fabricated by Hydrothermal Method Using Different Thicknesses of Seed Layers for Applications in Hybrid Photovoltaic Cells," Sensors and Materials, 28(5), 403-408.
3. Kamonchanok Roongraun, Navadol Laosiripojana, Surawut Chuangchote (2016) "Development of Photocatalytic Conversion of Glucose to Value-added Chemicals by Supported-TiO2 Photocatalysts," Applied Mechanics and Materials, 839, 39-43.
4. Mathana Wongaree, Siriluk Chiarakorn, Surawut Chuangchote, and Takashi Sagawa (2016) "Photocatalytic Performance of Electrospun CNT/TiO2 Nanofibers in a Simulated Air Purifier under Visible Light Irradiation," Environmental Science and Pollution Research, 23, 21395-21406.
5. Navaporn Kaerkitcha, Surawut Chuangchote, Kan Hachiya, and Takashi Sagawa (2017) "Influence of the Viscosity Ratio of Polyacrylonitrile/Poly(methyl methacrylate) Solutions on Core-Shell Fibers Prepared by Coaxial Electrospinning", Polymer Journal, 49, 497-502.
6. Jiraporn Payormhorm, Surawut Chuangchote, Kunlanan Kiatkittipong, Siriluk Chiarakorn, and Navadol Laosiripojana (2017) "Xylitol and Gluconic Acid Productions via Photocatalytic-Glucose Conversion Using TiO_2 Fabricated by Surfactant-Assisted Techniques: Effects of Structural and Textural Properties", Materials Chemistry and Physics, 196, 29-36.
7. Jiraporn Payormhorm, Surawut Chuangchote, and Navadol Laosiripojana (2017) "CTAB-Assisted Sol-microwave Method for Fast Synthesis of Mesoporous TiO_2 Photocatalysts for Photocatalytic Conversion of Glucose to Value-added Sugars", Materials Research Bulletin, 95, 546-555.
8. Nutsanun Klueb-arb, Surawut Chuangchote, Kamonchanok Roongraung, Navadol Laosiripojana, and Takashi Sagawa (2017) "Fabrication of Several Metal-Doped TiO_2 Nanoparticles and Their Physical Properties for Photocatalysis in Energy and Environmental Applications", Journal of Sustainable Energy & Environment, accepted.

Annual Activity Report on Japan-ASEAN Science, Technology and Innovation Platform (JASTIP), Work Package 2 (WP2) - Energy and Environment

P a g e 14 | 48

9. Puangphen Hongdilokkul, Surawut Chuangchote, Navadol Laosiripojana, and Takashi Sagawa (2017) "Conversion of Lignin via Photocatalysis Using Synthesized Ag-TiO$_2$ Photocatalysts Sintered under Different Atmospheres", Journal of Sustainable Energy & Environment, accepted.

1.5.2 Conference Proceeding

1. Navaporn Kaerkitcha, Surawut Chuangchote, Takashi Sagawa, Control of the physical properties of carbon nanofibers obtained from coaxial electrospinning of PAN and PMMA with adjustable inner/outer nozzle ends, EMN Hong Kong Meeting, Hong Kong, PRC, 2016/12/10.
2. Navaporn Kaerkitcha, Surawut Chuangchote, Takashi Sagawa, Control of the physical properties of carbon nanofibers obtained from coaxial electrospinning of PAN and PMMA with adjustable inner/outer nozzle ends, Ajou – Kyoto University Joint Symposium 2016, Swon, South Korea, 2016/1/28.
3. Navaporn Kaerkitcha, Surawut Chuangchote, Kan Hachiya, Takashi Sagawa, "Suitable outer/inner viscosity ratio of polymer solutions for fabrication of core-shell fibers by coaxial electrospinning," The 11th SPSJ International Polymer Conference (IPC2016), Fukuoka, 2016/12/16.
4. Kamonchanok Roongraun, Navadol Laosiripojana, and Surawut Chuangchote, 2015, "Development of Photocatalytic Conversion of Glucose to Value-added Chemicals by Supported-TiO2 Photocatalysts," World Future Alternatives (Naresuan University, Phitsanulok, November 30-December 2), School of Renewable Energy Technology.
5. Jiraporn Payormhorm, Xiaobo Li, Thomas Maschmeyer, Navadol Laosiripojana, and Surawut Chuangchote, 2016 "The Study of Photocatalytic Oxidation of Benzyl Alcohol with g-C3N4 under Visible Light: Effect of pH and Salt," 2016 5th International Conference on Material Science and Engineering Technology (ICMSET 2016) (Tokyo, Japan, October 29-31), University of Tokyo.
6. Patcha Pattanapibul, Surawut Chuangchote, Navadol Laosiripojana, Verawat Champreda, Jerawut Kaewsaenee, 2017 "Enhancement of Enzymatic Hydrolysis and Lignin Removal of Bagasse Using Photocatalytic Pretreatment," The 3rd International Conference on Renewable Energy Technologies (ICRET2017) (Thammasat University, Bangkok, Thailand, January 22-24), ICRET Organization.
7. Surawut Chuangchote, 2017 "Electrospun TiO$_2$ Nanofibers Composed of Bundle of Aligned Nanofibrils: Fabrication, Structural and Photoluminescent Properties," 11th South East Asean Technical University Consortium (Ho Chi Minh City University of Technology (HCMUT), Vietnam, March 13-15), Ho Chi Minh City University of Technology.
8. Puangphen Hongdilokkul, Surawut Chuangchote, Navadol Laosiripojana, Takashi Sagawa, 2017 "Effects of Sintering Conditions in Ag-TiO$_2$ Nanoparticles on Photocatalytic Degradation of Lignin," International Conference on Materials Processing Technology 2017 (MAPT 2017) (Ramada Plaza Bangkok Menam Riverside, Bangkok, November 30-December 1), King Mongkut's University of Technology Thonburi, NM_01.
9. Nutsanun Klueb-arb, Surawut Chuangchote, Navadol Laosiripojana, Takashi Sagawa 2017 "Modifications of TiO$_2$ Nanoparticle Catalysts by Dopes with Transition Metals (Ag and Cu) or Alkali Metal (Rb)," International Conference on Materials Processing Technology 2017 (MAPT 2017) (Ramada Plaza Bangkok Menam Riverside, Bangkok, November 30-December 1), King Mongkut's University of Technology Thonburi, NM_01.

1.5.3 Award

1. The Best Presentation Award in The 3rd International Conference on Renewable Energy Technologies (ICRET2017) (Ms. Patcha Pattanapibul).

1.5.4 Exchange Researches

Table 1. Exchange researches in JASTIP

Name	Exchange Period	Research Topic
Ms. Kamonchanok Roongraung	18 Feb 2016 - 19 July 2016	Nano-scaled Photocatalysts for Energy Applications
Mr. Suriyachai Nopparat	28 Sep 2016 - 31 May 2017	Modification of Visible Light Photocatalytic Activity for Biomass Conversion to Value-added Chemicals
Ms. Nutsanun Klueb-arb	14 Nov 2016 - 23 Dec 2016	A Study of Reaction Pathways in Photocatalytic Conversion of Sugars to High-Value Fuels and Chemicals
Ms. Puangphen Hongdilokkul	14 Nov 2016 - 23 Dec 2016	Photocatalytic Upgrading of Lignin to High Value Products by Nanostructured Catalysts
Ms. Kanyanee Sanglee	6 Feb 2017 - 17 Mar 2017	Development of Visible-Light Irradiation Responded Metal Oxide for Photocatalytic and Photovoltaic Applications
Ms. Nattida Srisasiwimon	29 May 2017 - 29 June 2017	Modification of Photocatalysts for Lignin Conversion
Ms. Oranoot Sittipunsakda	29 May 2017 - 29 June 2017	Development of Metal-doped Photocatalysts for Hydrogen Evolution

1.6   References

Awungacha, L. C., Hild, J., Czermak, P., and Herrenbauer, M. (2014). Photocatalytic active coatings for lignin degradation in a continuous packed bed reactor, *International Journal of Photoenergy*, *2014*.

Bahadur, N., Jain, K., Pasricha, R., and Chand, S. (2011), Selective gas sensing response from different loading of Ag in sol-gel mesoporous titania powders, *Sensors and Actuators B: Chemical*, **159**, 1, pp. 112-120.

Chaudhary, V., Srivastava, A.K., and Kumar, J. (2011), On the Sol-gel Synthesis and Characterization of Titanium Oxide Nanoparticles, *Materials Research Society*, **1352**.

Cheng, G., Akhtar, M.S., Yang, O.B., and Stadler, F.J. (2013), Structure modification of anatase TiO_2 nanomaterials-based photoanodes for efficient dye-sensitized solar cells, *Electrochimica acta*, **113**, pp. 527-535.

Annual Activity Report on Japan-ASEAN Science, Technology and Innovation Platform (JASTIP), Work Package 2 (WP2) - Energy and Environment

P a g e 16 | 48

Colmenares J.C., Magdziarz A., and Bielejewska A. (2011), High-value chemicals obtained from selective photo-oxidation of glucose in the presence of nanostructured titanium photocatalysts, *Bioresource Technology*, **102**, pp. 11254-11257.

Fan, H. X., Li, H. P., Liu, Z. H., Yang, F., and Li, G. (2015). Production of fine chemicals by integrated photocatalytical degradation of alkali lignin solution in corrugated plate reactor and cyclic extraction technology, *Industrial Crops and Products*, *74*, 497-504.

Gomathisankar, P., Yamamoto, D., Katsumata, H., Suzuki, T., and Kaneco, S. (2013), Photocatalytic hydrogen production with aid of simultaneous metal deposition using titanium dioxide from aqueous glucose solution, *International Journal of Hydrogen Energy*, **38**, pp. 5517-5524.

Hwang, K.J., Lee, J.W., Shim, W.G., Jang, H.D., Lee, S.I., and Yoo, S.J. (2012), Adsorption and photocatalysis of nanocrystalline TiO_2 particles prepared by sol-gel method for methylene blue degradation, *Advance Powder Technology*, **23**, pp. 414-418.

Jaimy, K. B., Vidya, K., Saraswathy, H. U. N., Hebalkar, N. Y., and Warrier, K. G. K. (2014), Dopant-free anatase titanium dioxide as visible-light catalyst: Facile sol-gel microwave approach, *Journal of Environmental Chemical Engineering*.

Li, H., Lei, Z., Liu, C., Zhang, Z., and Lu, B. (2015). Photocatalytic degradation of lignin on synthesized Ag–AgCl/ZnO nanorods under solar light and preliminary trials for methane fermentation, *Bioresource Technology*, *175*, 494-501.

Mozia S., Heciak A., and Morawski A.W. (2011), Photocatalytic acetic acid decomposition leading to the production of hydrocarbons and hydrogen on Fe-modified TiO_2, *Catalysis Today*, **161**, pp. 189-195.

Murugan, K., Subasri, R., Rao, T.N., Gandhi, A.S., and Murty, B.S. (2013), Synthesis, characterization and demonstration of self-cleaning TiO_2 coatings on glass and glazed ceramic tiles, *Progress in Organic Coatings*, **76**, pp. 1756-1760.

Mutuma, B. K., Shao, G. N., Kim, W. D., and Kim, H. T. (2015), Sol-gel synthesis of mesoporous anatase-brookite and anatase-brookite-rutile TiO_2 nanoparticles and their photocatalytic properties, *Journal of colloid and interface science*, **442**, pp. 1-7.

Nasralla, N., Yeganeh, M., Astuti, Y., Piticharoenphuna, S., Shahtahmasebi, N., Kompany, A., Karimipour, M., Mendis, B.G., Poolton, N.R.J., Siller, L., 2013, "Structural and spectroscopic study of Fe-doped TiO_2 nanoparticles prepared by sol–gel method", **Scientia Iranica**, Vol. 20, pp. 1018-1022.

Oh, J. K., Lee, J. K., Kim, S. J., and Park, K. W. (2009), Synthesis of phase- and shape-controlled TiO_2 nanoparticles via hydrothermal process, *Journal of Industrial and Engineering Chemistry*, **15**, 2, pp. 270-274.

Prado, R., Erdocia, X., and Labidi, J. (2013). Effect of the photocatalytic activity of TiO_2 on lignin depolymerization, *Chemosphere*, *91*(9), 1355-1361.

Park, J.Y., Yun, J.J., Hwang, C.H., and Lee, I.H. (2010), Influence of silver doping on the phase transformation and crystallite growth of electrospun TiO_2 nanofibers, *Materials Letters*, **64**, pp. 2692-2695.

Shen, X., Zhang, J., and Tian, B. (2011), Microemulsion-mediated solvothermal synthesis and photocatalytic properties of crystalline titania with controllable phases of anatase and rutile, *Journal of hazardous materials*, **192**, 2, pp. 651-657.

Shi, J., & Wang, X. (2011). Growth of rutile titanium dioxide nanowires by pulsed chemical vapor deposition. *Crystal Growth & Design*, *11*(4), 949-954.

Shojaie, A.F., and Loghmani, M.H. (2010), La^{3+} and Zr^{4+} co-doped anatase nano TiO$_2$ by sol-microwave, *Chemical Engineering Journal*, **157**, pp. 263-269.

Song, S., Yang, T., Li, Y., Pang, Z., Lin, L., Lv, M., and Han, S. (2009), Structural, electrical and optical properties of ITO films with a thin TiO$_2$ seed layer prepared by RF magnetron sputtering, *Vacuum*, **83**, 8, pp. 1091-1094.

Su, C., Hong, B.Y., and Tseng, C.M. (2004), Sol-gel preparation and photocatalysis of titanium dioxide, *Catalysis today*, **96**, pp. 119-126.

Suwarnkar, M. B., Dhabbe, R. S., Kadam, A. N., & Garadkar, K. M. (2014). Enhanced photocatalytic activity of Ag doped TiO$_2$ nanoparticles synthesized by a microwave assisted method. *Ceramics International*, *40*(4), 5489-5496.

Tahir, A.A., Peiris, T.A., and Wijayantha, K.G. (2012), Enhancement of Photoelectrochemical Performance of AACVD-produced TiO$_2$ Electrodes by Microwave Irradiation while Preserving the Nanostructure, *Chemical Vapor Deposition*, **18**, 4-6, pp. 107-111.

Tanaka, Y., Sakai, H., Tsuke, T., Uesugi, Y., Sakai, Y., and Nakamura, K. (2011), Influence of coil current modulation on TiO$_2$ nanoparticle synthesis using pulse-modulated induction thermal plasmas, *Thin Solid Films*, **519**, 20, pp. 7100-7105.

Tobaldi, D. M., Škapin, A. S., Pullar, R. C., Seabra, M. P., & Labrincha, J. A. (2013). Titanium dioxide modified with transition metals and rare earth elements: phase composition, optical properties, and photocatalytic activity.*Ceramics International*, *39*(3), 2619-2629.

Vijayalakshmi, R., and Rajendran, V. (2012), Synthesis and characterization of nano-TiO$_2$ via different methods, *Arch App Sci Res*, **4**, 2, pp. 1183-1190.

Zhang, Y., Zheng, H., Liu, G., and Battaglia, V. (2009), Synthesis and electrochemical studies of a layered spheric TiO$_2$ through low temperature solvothermal method, *Electrochimica Acta*, **54**, 16, pp. 4079-4083.

Zhao, Y., Li, C., Liu, X., Gu, F., Jiang, H., Shao, W., and He, Y. (2007), Synthesis and optical properties of TiO$_2$ nanoparticles, *Materials Letters*, **61**, 1, pp. 79-83.

Annual Activity Report on Japan-ASEAN Science, Technology and Innovation Platform (JASTIP),
Work Package 2 (WP2) - Energy and Environment

P a g e 18 | 48

Development of Carbons from Biomass

for Energy Storage Applications

Annual Activity Report on Japan-ASEAN Science, Technology and Innovation Platform (JASTIP),
Work Package 2 (WP2) - Energy and Environment

P a g e 19 | 48

2. Development of Carbons from Biomass for Energy Storage Applications

Research team:

Dr. Sumittra Charojrochkul, MTEC, NSTDA (Project leader, Thai side)

Prof. Dr. Takeshi Abe, Kyoto University (Project leader, Japan side)

Dr. Yatika Somrang, MTEC, NSTDA

Dr. Yuto Miyahara, Kyoto University

Dr. Pannipa Tepamat, Thammasat University

Mr. Thanathon Sesuk, MTEC, NSTDA

2.1 Introduction

Thailand is an agricultural-based country which produces large amount of biomass but the majority of this abundant resources, especially agricultural leftover, has not yet been exploited extensively. Currently, the use of biomass in fuel application has been widely studied and practiced in order to reduce the reliance on petroleum-derived fuels. Not only its benefit as a substitute to conventional fuels, but bio-based economy can also be developed based on biomass. Biomass which mainly contains cellulose, hemicellulose and lignin can be converted into chemicals or valuable products. In fact, biomass is a major carbon source which can potentially be used in energy storage devices. Recently, there have been many previous works investigating the potential of using biomass as a source to produce carbons from carbonisation/hydrothermal carbonisation and/or chemical activation for energy storage application. However, none of the work has attempted to comprehend the effect of biomass constituents on the electrochemical characteristics for energy storage devices. In addition, the production of high-quality carbon materials from 'challenging' biomass, i.e. ash-containing biomass, particularly palm empty fruit bunch (PEFB), has not yet well established. This project, hence, aims to understand the role of precursor constituents on the electrochemical properties of the carbons and to develop method/conditions for the activated carbon production from palm empty fruit bunch using carbonisation/hydrothermal and/or chemical activation. This work is jointly collaborated between MTEC/NSTDA, responsible for producing carbon from biomass and performing physical characterisation of the obtained carbon, and Kyoto University, in charge of conducting electrochemical characterisation of the carbons for lithium-ion battery and supercapacitor applications.

Annual Activity Report on Japan-ASEAN Science, Technology and Innovation Platform (JASTIP), Work Package 2 (WP2) - Energy and Environment

P a g e 20 | 48

2.2 Research Progress
2.2.1 Effect of activation temperature and KOH/C ratio

Carbons were produced at different activation temperature and KOH/C ratio. At KOH/C = 1, surface area of carbon produced at 700-900 °C are insignificantly different. However, as per pore size distribution, the pore width of micropore decreases with increasing temperature as shown in Figure 1a. This causes shorter duration time of charge cycle (Figure 1b) and less capacitance (Figure 1c) in the 700 °C carbon than those produced at higher temperatures. Figure 1c also shows that increasing activation temperature improves rate capability.

a)

b)

c)
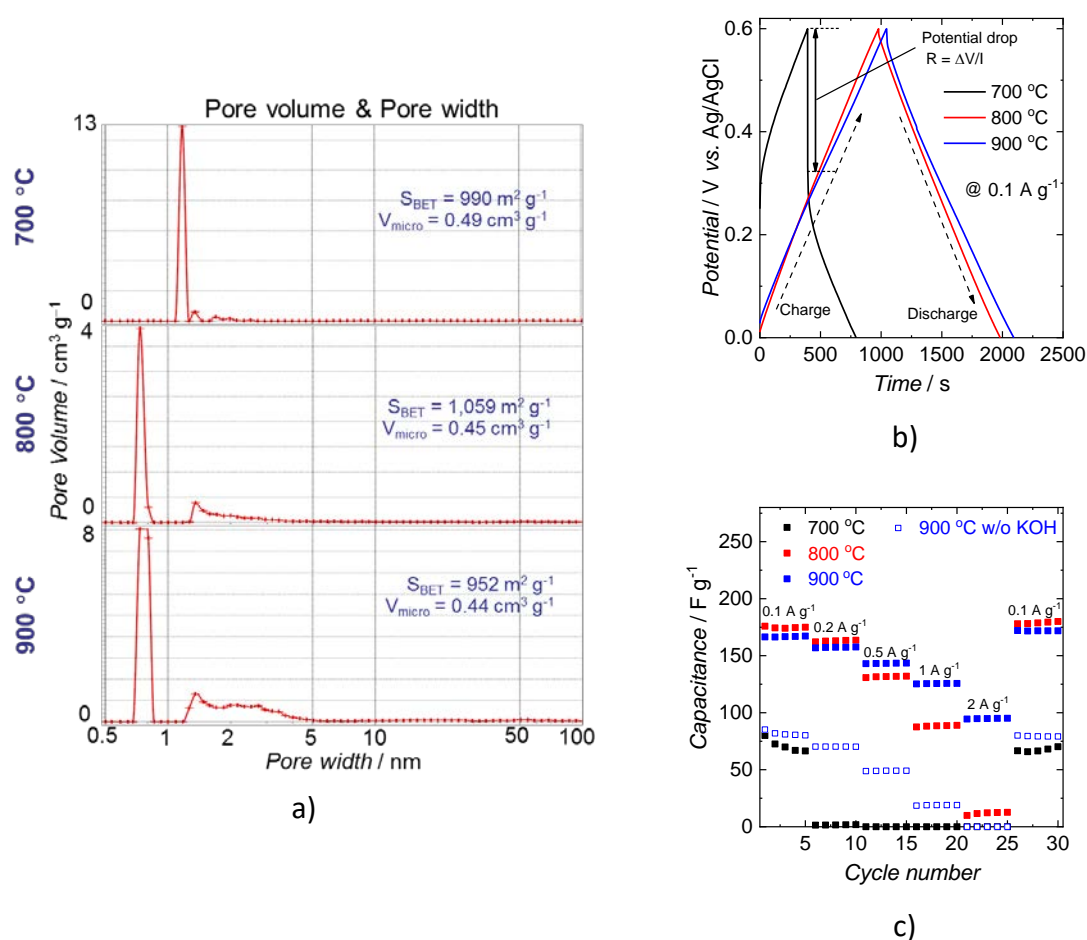
Figure 1 Physical and electrochemical properties of carbon produced at KOH/C = 1. a) Surface area and pore size distribution; b) Potential profile vs. time; c) Capacitance at different current density

Annual Activity Report on Japan-ASEAN Science, Technology and Innovation Platform (JASTIP),
Work Package 2 (WP2) - Energy and Environment

P a g e 21 | 48

At KOH/C = 3, increasing temperature improves both surface area and occurrence of mesopore as shown in Figure 2a. The charge cycle time of carbon produced at 700-900 °C (Figure 2b) are comparable while the rate capability improves with increase temperature as also observed at KOH/C = 1. However, severe temperature (1,100 °C) results in crystalline structure (Figure 2d) and the EDLC performance of carbon appears to deteriorate.
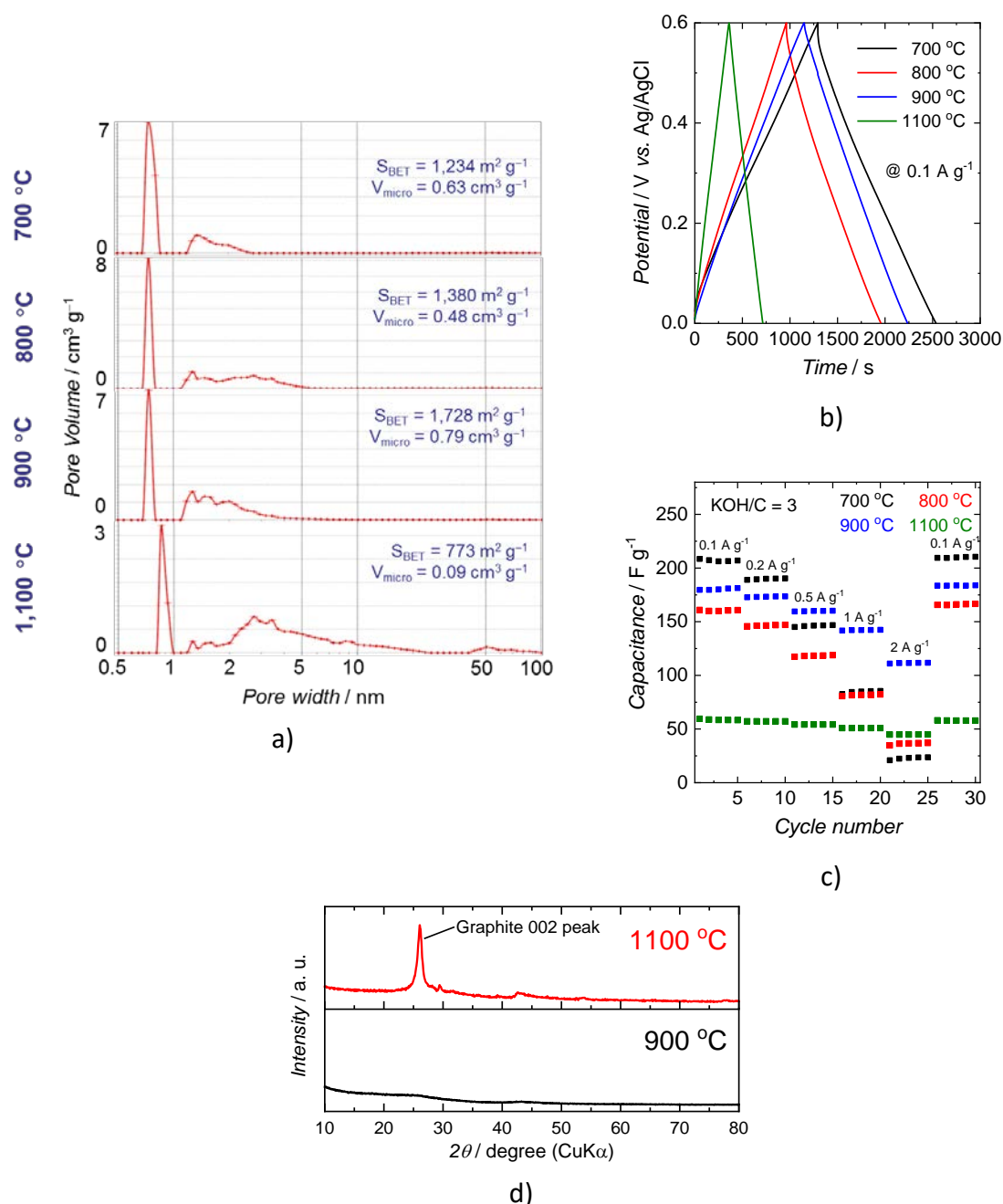
Figure 2 Physical and electrochemical properties of carbon produced at KOH/C = 3. a) Surface area and pore size distribution; b) Potential profile vs. time; c) Capacitance at different current density; d) XRD spectra

Annual Activity Report on Japan-ASEAN Science, Technology and Innovation Platform (JASTIP),
Work Package 2 (WP2) - Energy and Environment

P a g e 22 | 48

Annual Activity Report on Japan-ASEAN Science, Technology and Innovation Platform (JASTIP), Work Package 2 (WP2) - Energy and Environment

P a g e 23 | 48

2.2.2 Effect of KOH-mixing sequence

Carbons were produced at different KOH-mixing sequence, i.e. KOH-Carbonisation-Activation (KCA) and Carbonisation-KOH-Activation (CKA). It can be observed that KCA yields better surface area and pore size distribution (high mesopore and smaller pore width of micropore) as shown in Figure 3a. This results in longer charge cycle time (Figure 3b). Moreover, as for KCA process, carbonisation at 500 °C appears to yield carbon with better pore morphology and, thus, electrochemical properties than that at 300 °C.
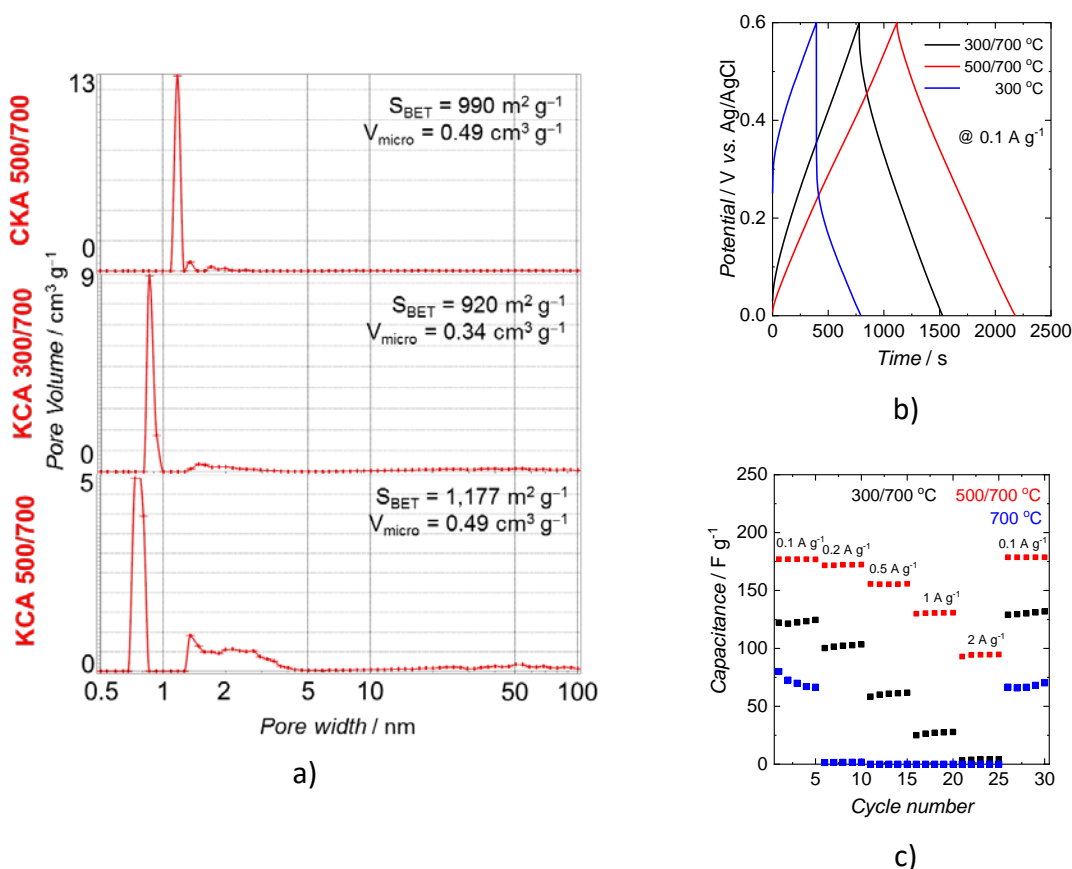
Figure 3 Physical and electrochemical properties of carbon produced with different KOH-mixing sequence. a) Surface area and pore size distribution; b) Potential profile vs. time; c) Capacitance at different current density

2.3 Project Output

2.3.1 Student exchange

- Two students from Thammasat University visited Kyoto University under the W&W Internship program in January 2018.

Annual Activity Report on Japan-ASEAN Science, Technology and Innovation Platform (JASTIP),
Work Package 2 (WP2) - Energy and Environment

P a g e 25 | 48

Innovations in Biomass Application for Catalytic Material Synthesis and Energy Devices

Annual Activity Report on Japan-ASEAN Science, Technology and Innovation Platform (JASTIP),
Work Package 2 (WP2) - Energy and Environment

P a g e 26 | 48

3. Innovations in Biomass Application for Catalytic Material Synthesis and Energy Devices

Research team:

Assoc.Prof.Dr. Noriaki Sano, Kyoto University (PI, Japan side)

Dr. Kajornsak Faungnawakij, NANOTEC, NSTDA (PI, Thailand side)

Dr. Vorranutch Itthibenchapong, NANOTEC, NSTDA

Dr. Pongtanawat Khemthong, NANOTEC, NSTDA

Dr. Sanchai Kuboon, NANOTEC, NSTDA

Dr. Supawadee Namuangruk, NANOTEC, NSTDA

Dr. Chompoonut Rungnim, NANOTEC, NSTDA

Dr. Pussana Hirunsit, NANOTEC, NSTDA

Dr. Chalida Klaysom, Chulalongkorm University

Assoc.Prof. Tawatchai Charinpanitkul, Chulalongkorm University

Dr. Sareeya Bureekaew, VISTEC

Miss. Chuleeporn Luadthong, NANOTEC, NSTDA

Miss. Rungnapa Kaewmeesri, NANOTEC, NSTDA

3.1 Purpose of Collaborative Research

The catalytic production of carbon-based materials, biofuels and biochemicals is a key activity in biorefinery industry. Also, developments in catalytic energy conversion and energy storage using bioactivities are important for sustainable societies. Consequently, searching for renewable resources that are reliable, sustainable and environmentally friendly is the big challenge, and these lead to green concepts including biorefinery and bio-energy devices where renewable resources drive the world. Under such circumstances, the collaborative researches carried out by the groups in NANOTEC/NSTDA (Faungnawakij's team) and Kyoto University (Sano's team) will attack this issue via accumulating innovative knowledge about biomass conversion to useful materials and development of bio-energy devices.

In this year, three major research activities have been done as follows.

- Development of carbon-based catalysts for conversion of biomass derivatives to γ-valerolactone (GVL)
- Development of ultra-fast method to prepare activated carbon using microwave irradiation into KOH activation
- Development of Fe-dispersed carbon nanohornsnrs for H2 storage–carbon nanohorns dispersed with Fe nanoparticles have been developed, and its H2 storage mechanism has been investigated by molecular orbital calculation

Annual Activity Report on Japan-ASEAN Science, Technology and Innovation Platform (JASTIP),
Work Package 2 (WP2) - Energy and Environment

P a g e 27 | 48

3.2 Research Progress

3.2.1 Development of carbon-based catalysts for conversion of biomass derivatives to γ-valerolactone (GVL)

γ-valerolactone (GVL) is a fine chemical which is widely used as a green solvent, a fuel additive and a green fuel. It can be produced from lignocellulosic biomass and its derivatives, such as methyl levulinate (ML) via catalytic hydrogenation reaction. In this work, novel hybrid materials of Ni nanoparticles and single-walled carbon nanohorns (Ni/CNHs) synthesized from gas-injected arc-in-water (GI-AIW) method was used as catalysts for producing GVL from ML. Effect of surface modification, oxidation and reduction of Ni/CNHs on their catalytic activity was investigated. For comparison of catalytic activities, Ni on other carbon supports prepared by the conventional wet impregnation and unsupported Ni catalysts were examined. X-ray diffractometry (XRD), transmission electron microscopy (TEM), field-emission scanning electron microscopy (FE-SEM), N_2 sorption, thermogravimetric analysis (TGA), Hydrogen-temperature-programmed reduction (H_2-TPR), and Fourier Transform Infrared (FT-IR) spectroscopy were employed for elucidating different characteristics of all examined catalysts. It was found that reduced oxidized Ni/CNHs exhibited the highest catalytic performance with 96% conversion of ML, 90% yield, and 93 % selectivity of GVL.

1. Introduction

γ-valerolactone (GVL) is a high value-added chemical which is widely used as a green solvent, fuel additive, as well as a raw material for producing long chain alkanes [1-4]. It can be synthesized by catalytic hydrogenation of methyl levulinate (ML), which is derived from lignocellulosic biomass. Generally, hydrogen gas (H_2) could be easily supplied for the catalytic hydrogenation of ML with high selectivity. Nevertheless, liquid-phased hydrogenation or transfer hydrogenation making use of liquid solvents as hydrogen donors is also another preferable alternative. In such a transfer hydrogenation process, hydrogen is supplied by H-donor solvents, such as liquid alcoholic compounds [5, 6]. Therefore, the transfer hydrogenation of ML to produce GVL with either homogenous or heterogeneous catalysts have been studied [7]. It should be noted that heterogeneous catalysts are recognized as an attractive option because they are easier to be handled or recycled, and more environmental friendly [5, 7, 8]. Recently, many researchers have reported that Ru-C composites could provide promising catalytic activity for ML conversion [4, 5, 9, 10]. Other noble metals, for instance Pt, Pd, and Rh with or without support materials have also been investigated for hydrogenation reaction [11]. On the other hand, other cheaper transition metals with potential for catalyzing hydrogenation reaction have recently gained increasing research interest. Among various transition metals, Ni is well known as a promising catalyst for hydrogenation reaction. Therefore, Ni and Ni-based alloys with or without support materials have been examined as a catalyst for hydrogenation of various cellulosic compounds [1, 2, 12].

Single-walled carbon nanohorns (CNHs) are carbon nanostructures with unique properties when compared to other nanomaterials. CNHs possess large specific surface area, excellent conductivity, and high chemical stability [13, 14]. As a result, CNHs have been used in many applications, such as electrodes, biosensors, catalyst supports and gas storage [15-17]. Among

Annual Activity Report on Japan-ASEAN Science, Technology and Innovation Platform (JASTIP),
Work Package 2 (WP2) - Energy and Environment

P a g e 28 | 48

various synthesizing methods, gas-injected arc-in-water (GI-AIW) is a simple method to produce various carbon nanoparticles. Moreover, GI-AIW can be applied to synthesize other hybrid materials of metal and carbonaceous nanostructures within a single-step [18]. Especially, Ni, Pd, Pt hybridized with carbon nanohorns could be fabricated by this method instead of using other conventional means, such as wet impregnation.

In addition, surface modification is an important mean to provide adjustable effect on characteristics and performance of particulate catalysts. Oxidation process is commonly applied to modify the surface of carbon nanomaterials, especially increasing their specific surface area and attaching some specific functional groups [19-21]. On the other hand, reduction process has been used for controlling the phase of metals and metal oxides, which could consequently affect the surface property of such metallic nanoparticles. Poonjarernsilp et al. [22] reported that liquid phase oxidation could provide sulfonated CNHs which were effective for esterification of palmitic acid. Meanwhile, Oliveira et al. [23] reported that the activation using H2 could affect the specific surface area of activated carbons. However, to the best of our knowledge, modification of Ni/CNHs which could be employed as a catalyst for hydrogenation of ML have not been explored and clearly understood yet.

The objective of this work was to investigate the performance of the novel catalysts which were Ni hybridized with single-walled carbon nanohorns for converting ML to GVL. Ni on activated carbon, Ni on multi-walled carbon nanotube, NiO, and Ni catalysts were examined under an identically regulated condition to compare their catalytic performance. Finally, reusability of reduced and oxidized Ni hybridized with CNHs and effect of reaction temperature on conversion of ML, yield, and selectivity of GVL were examined regarding to characteristics of fresh and used catalysts.

2. Experimental

2.1 Catalyst preparation

2.1.1 Preparation of Ni/CNHs using gas-injected arc-in-water method and surface modification

Ni hybridized with carbon nanohorns (Ni/CNHs) were synthesized using gas-injected arc-in-water (GI-AIW) method which could also enable various metal nanoparticles to be hybridized with carbon nanohorns as explained in details elsewhere [24]. In short, a graphite rod with a diameter of 20 mm and a length of 55 mm was used as a cathode. An anode was made of a hollow graphite rod with an outer diameter of 6 mm, an inner diameter of 1.5 mm, and a length of 75 mm with a hole depth of 7 mm. 10 pieces of Ni wires (Nilaco cooperation) with a diameter of 0.03 mm were twisted and inserted into a center-hold of the graphite anode. A set of the cathode and the anode was submerged in de-ionized water contained in a beaker. Direct electrical current of 80 amperes was supplied from a power source for generating arc discharge between both electrodes. The anode was moved toward the inner surface of the cathode hole by a step motor with a speed of 5.25 mm/s. Synthesized product was collected after being dried in an oven set at 90 °C overnight. Such synthesized product was notified as Ni/CNHs.

To modify their surface property, Ni/CNHs were either oxidized or reduced as well as being oxidized and then reduced later. Oxidation of 0.5 g Ni/CNHs was conducted in a tubular reactor under the atmospheric pressure and 380 °C for 15 min. After cooling down, oxidized Ni/CNHs (oxd-Ni/CNHs) were collected with an average yield of 65 wt%. The reduction process was also performed in the tubular reactor under H_2 atmosphere. Ni/CNHs sample (0.2 g) was put in a ceramic boat placed in the tubular reactor. 0.1 ml/min H_2 flow was supplied into the reactor for 30 min to flush remaining air out of the reactor. Then, the H_2 flow rate was decreased to 0.01 ml/min, and the reactor was heated up to 500 °C and kept constant for 1 h. Finally, N_2 with a flow rate of 0.1 ml/min was fed to cool down the products which were assigned as reduced Ni/CNHs (red-Ni/CNHs). The average yield of red-Ni/CNHs was 75 wt%. The combined oxidation-reduction treatment of Ni/CNHs was also conducted by the same procedures with a sequence of oxidation and reduction respectively, resulting in the samples of reduced and oxidized Ni/CNHs (red-oxd-Ni/CNHs).

2.1.2 Preparation of other catalysts by wet impregnation method

$Ni(NO_3)_2 \cdot 6H_2O$ (Quality Reagent Chemical) with a stoichiometrically prepared amount was used as an aqueous precursor for impregnation of 20 wt% Ni onto each carbonaceous support material. Activated carbon (Sigma-Aldrich) and multi-walled carbon nanotubes (Bayer Material Science) were used as support materials. Each resultant sample was dried in a vacuum oven at a temperature of 80 °C overnight. Finally, the resultant sample was calcined and reduced using the similar oxidation and reduction processes as mentioned above. Ni catalyst impregnated on activated carbon and Ni catalyst impregnated on multi-walled carbon nanotubes were assigned as Ni/AC and Ni/CNTs, respectively.

Moreover, Ni and NiO catalysts without carbon support material were also prepared and used in the control experiments. NiO catalysts were simply synthesized by annealing $Ni(NO_3)_2 \cdot 6H_2O$ in an electric furnace at 700 °C for 5 h with a heating rate of 10 °C/min. The greenish appearance of resultant samples could confirm the formation of NiO. Then NiO samples were further reduced in a tubular reactor by the same reduction process to prepare metallic Ni catalyst samples. The black powdery appearance could also confirm the presence of metallic Ni in the resultant samples.

2.2. Catalyst characterization

Crystallographic identification of each typical catalyst was performed by X-ray diffractometry (XRD, Bruker, D8 advance) using CuKα radiation operated at 40 kV and 100 mA with a scanning step of 0.03 °/min in a range of 10° to 90°. Samples were prepared using Si low background as a sample holder.

Morphology, dispersion, and size distribution of metallic species within each catalyst sample were investigated by transmission electron microscope (TEM, JEOL, JEM-2100Plus) and field-emission scanning electron microscope (FE-SEM, Hitachi, S8030). Size distribution of Ni nanoparticles embedded in each carbonaceous support material was analyzed from substantial TEM

Annual Activity Report on Japan-ASEAN Science, Technology and Innovation Platform (JASTIP), Work Package 2 (WP2) - Energy and Environment

P a g e 30 | 48

micrographs by ImageJ software. In addition, Ni content in each sample was determined by energy-dispersive X-ray spectroscopy (EDX) equipped with FE-SEM.

BET surface area of each carbonaceous support material and catalyst samples was characterized by N2 sorption (Bel Japan, BELSORP-miniII). Brunauer–Emmett–Teller (BET) equation was used to determine the specific surface area of each sample.

Thermal stability analysis of each catalyst sample was conducted by thermogravimetric analyzer (TGA, PerkinElmer, TGA 8000). Sample of each catalyst placed in a ceramic pan was heated in an oxygen flow from the ambient temperature up to 900 °C with a heating rate of 10 °C/min. Ni content was determined from the TGA result based on the assumption that Ni species in the sample was completely oxidized into NiO.

Hydrogen-temperature-programmed reduction (H2-TPR) analysis of each catalyst was performed using chemisorption analyzer (Quantachrome, ChemStar) equipped with a thermal conductivity detector to confirm the reduction behaviors of the catalyst. 45 mg of each catalyst was put in a U-tube sample cell and then pretreated under He atmosphere at 150 °C for 1 h. After being purged by Ar flow for 30 min and cooled down to 50 °C, the catalyst sample was heated again to 900 °C with a heating rate of 5 °C/min in a 5% H2/Ar flow.

Functional groups on the surface of Ni/CNHs catalysts treated with different thermal conditions were examined by FT-IR spectroscopy (Thermo Scientific, Nicolet6700). As a standard procedure, each sample was mixed with KBr and compressed into a thin pellet before being analyzed by the infrared irradiation in a 4000-500 cm-1 wavenumber region.

2.3. Catalytic performance measurement

To evaluate the catalytic performance of the catalysts, hydrogenation of methyl levulinate (ML) to convert to γ-valerolactone (GVL) in batch reactor was tested. As a general procedure, 0.1 g of each catalyst and 24 cm3 of 0.2 M methyl levulinate in 2-propanol were mixed under continuous magnetic stirring. Conversion of ML was initiated by heating with a heating rate of 10 °C/min and then kept at a designated temperature for 3 h. Then, the liquid product was collected and analyzed by gas chromatography (GC, Shimadzu, GC-2010 Plus equipped with DB-WAX Column). Effect of reaction temperature at 140, 170, and 200 °C on the performance of the catalyst was examined. In addition, reusability of the catalyst was investigated by comparison of the performance of the used catalyst. The used catalyst was recovered by filtration and dried overnight in a vacuum oven at 60 °C before being tested in converting ML again for 5 repetitive cycles. The ML conversion, GVL yield and selectivity were determined by the following equations:

$$\text{ML conversion (\%)} \quad = \quad \frac{\text{Mole of ML reacted}}{\text{Mole of initial ML}} \times 100 \qquad (1)$$

$$\text{GVL yield (\%)} \quad = \quad \frac{\text{Mole of GVL produced}}{\text{Mole of initial ML}} \times 100 \qquad (2)$$

$$\text{GVL selectivity (\%)} = \frac{\text{Mole of GVL produced}}{\text{Mole of ML reacted}} \times 100 \qquad (3)$$

3. Results and discussion

3.1. Characterization of each carbonaceous support material and catalyst sample

Fig. 1 presents XRD patterns of all carbonaceous support materials (carbon nanohorns (CNHs), carbon nanotubes (CNTs) and activated carbon (AC)) and all synthesized catalysts. A characteristic peak at 2θ of about 26.8 representing graphite structure was detected in all carbonaceous support materials as shown in Fig. 1(a). In Fig. 1(b), diffraction peaks at 2θ = 44.5° and 51.8°, which represent Ni(111) and Ni(200) planes, respectively, as well as diffraction peaks at 2θ = 37.2°, 43.3°, and 62.9°, which represent NiO(111), NiO(200), and NiO(220) plains of NiO, respectively could be detected in all resultant Ni/CNHs hybrid catalysts [25]. Similar diffraction peaks were also detected for Ni, NiO, Ni/AC and Ni/CNTs samples as illustrated in Fig. 1(c). Appearance of the characteristic peaks of Ni in all Ni/CNHs, red-Ni/CNHs, oxd-Ni/CNHs, red-oxd-Ni/CNHs, Ni/AC, Ni/CNTs samples could confirm the success of embedding Ni onto each carbonaceous support material. It should be noted that the characteristic peaks at 2θ = 37.2°, 43.3°, and 62.9° were clearly detected in the oxd-Ni/CHN samples, which could confirm the partial oxidation of Ni. More interestingly, Fig. 1(d) reveals that the diffraction peaks of Ni(111) and Ni(200) at 2θ = 44.5° and 51.8°, could be detected in fresh red-oxd-Ni/CNHs sample and red-oxd-Ni/CNHs sample incorporated in hydrogenation of ML. These results would suggest that Ni crystalline in the red-oxd-Ni/CNHs catalyst was not affected by the transfer hydrogenation of ML.

TEM analyses were used to investigate morphology and size distribution of Ni nanoparticles embedded in CNH and CNT support materials. TEM micrographs of CNHs, Ni/CNHs treated with different thermal conditions, and Ni/CNTs are presented in Fig. 2(a)-(g), respectively. Fig. 2(a) reveals that the synthesized CNHs contain only carbon species without any contamination of other species. Comparison of Fig. 2(b), (c), (f), and (g) suggests that the embedded Ni nanoparticles were uniformly dispersed within the CNHs. The treatment by oxidation or reduction exerted insignificant effect on the morphology of Ni/CNHs. However, the average size of Ni nanoparticles was slightly increased after Ni/CNHs were subjected to oxidation and reduction. These results would be ascribed that the consecutive treatment of Ni/CNHs by oxidation and reduction would inevitably result in sintering of Ni nanoparticles [12]. In addition, comparison of Fig. 2 (c) and (d) suggests that the average size of Ni nanoparticles in the used red-oxd-Ni/CNHs is almost equivalent to that in the fresh red-oxd-Ni/CNHs. Incorporating of this information and the results of XRD analyses would suggest that the red-oxd-Ni/CNHs exhibited an excellent stability. As confirmed by particle size analyses, the average size of Ni nanoparticles in Ni/CNTs shown in Fig. 2(e) was 15.2 nm, which was significantly larger than that in the red-oxd-Ni/CNHs.

For further confirmation, dispersion of Ni nanoparticles in Ni/AC and Ni/CNTs was analyzed using FE-SEM. As showed in Fig. 3 (a)-(c), Ni nanoparticle dispersion of Ni/CNHs was not affected by the thermal treatment by oxidation and reduction of Ni/CNHs. In addition, Fig. 3(c) and (d) reveal that Ni nanoparticles in the used red-oxd-Ni/CNHs were still uniformly dispersed as compared with those in the fresh red-oxd-Ni/CNHs. However, agglomeration of Ni nanoparticles could be

Annual Activity Report on Japan-ASEAN Science, Technology and Innovation Platform (JASTIP),
Work Package 2 (WP2) - Energy and Environment

P a g e 32 | 48

observed in Ni/AC as shown in Fig. 3 (e). In addition, partial agglomeration of Ni nanoparticles in Ni/CNTs could be confirmed by FE-SEM analysis shown in Fig. 3 (f). It is noteworthy that dispersion of Ni nanoparticles in each sample confirmed by XRD analyses and microscopic analyses were in a reasonable agreement.

In general, agglomeration of Ni nanoparticles would result in lower active sites which are essential for ensuring good catalytic performance. Based on all of our microscopic analyses, dispersion of Ni nanoparticles within the pristine Ni/CNHs and Ni/CNHs with surface modification was similar because the structure of CNHs could act as a barrier to prevent Ni agglomeration. On the contrary, Ni nanoparticles which embedded on the surface of CNTs and AC exhibited a certain level of agglomeration. Moreover, there is much more agglomeration of Ni or NiO nanoparticles synthesized without using any support materials. These results would suggest that CNHs were a good candidate of support materials for accommodating catalytic nanoparticles with low agglomeration.

For quantitative analyses, N2 sorption was performed to measure BET surface area of all catalyst samples in comparison with that of carbonaceous support materials as summarized in Table 1. It was found that incorporation of Ni species onto CNHs could result in a decrease in BET surface area of Ni/CNHs when compared to that of the pristine CNHs. This is attributed to the lower BET surface area of Ni nanoparticles when compared to that of CNHs. Interestingly, the BET surface area of treated Ni/CNHs became approximately 2 folds higher than that of pristine Ni/CNHs. All treated Ni/CNHs possessed the specific surface area higher than 200 m2/g. However, treatment by oxidation, reduction, as well as oxidation following by reduction resulted in an insignificant difference in the BET surface area of those samples. Sano et al. ever reported that oxidation process could result in partial loss of carbonaceous content in CNHs due to the formation of carbon dioxide, resulting in an increase in the BET surface area of oxidized CNHs [26]. Therefore, after oxidation process, yield of the resultant catalyst was decreased due to the loss of reactive carbonaceous content [20, 27]. BET surface area of Ni/AC sample was much lower than that of AC sample because Ni nanoparticles, which would be dispersed onto the AC surface, tended to block the porous structure of AC, as observed by SEM analysis (Fig. 3 (e)). After impregnating Ni nanoparticles onto CNTs, the BET surface area of Ni/CNTs was slightly higher when compared to that of CNTs due to the contribution of Ni nanoparticles.

In addition, Ni content in each sample was also confirmed by EDX and TGA analyses as summarized in Table 1. It should be noted that Ni content was determined by SEM-EDX area-based analysis and TGA with assumption that carbon was not lost during the Ni-loading process. It could be confirmed that there was no Ni contained in the pristine CNHs, activated carbon and CNTs. In Ni/CNHs, 15 and 21 wt% Ni contents were estimated based on SEM-EDX surface-based and TGA analyses, respectively. It should be noted that Ni content evaluated by SEM-EDX surface-based analysis was lower than that of TGA result due to the difference in surface-based and volume-based analyses. Based on TGA results, Ni content within red-Ni/CNHs, oxd-Ni/CNHs and red-oxd-Ni/CNHs was 25, 33 and 36 wt%, respectively. In the samples of Ni/AC and Ni/CNTs, the stoichiometric estimation suggested the same Ni content of 20 wt%. Again the SEM-EDX surface-based analyses indicated that there were 28 and 15 wt% Ni in Ni/AC and Ni/CNTs, respectively. Finally, in the samples of NiO and metallic Ni, the SEM-EDX surface-based analysis revealed that there was the Ni content of 80 and 100 wt%, respectively. In addition, stability of Ni/CNHs treated with different conditions was confirmed by TGA and showed in the supporting material (S.01). All

of these results would suggest that the reduction and oxidation process exerted insignificant effect on the loss of Ni nanoparticles which were embedded in the CNHs. Therefore, these results suggest that all catalysts were thermally stable during the conversion of ML which was operated at much lower temperature.

For further confirmation of the presence of NiO within each typical sample, H2-TPR analytical results were compared in Fig. 4. For the samples of Ni/CNHs and red-Ni/CNHs, two distinctive peaks were detected at ~220 and 400 °C. The first peak reveals an increase in relative thermal conductivity difference (%TCD) which was corresponding to the reduction of NiO while the second peak reflected gasification of carbon content [28, 29]. These H2-TPR results could confirm the presence of NiO species instead of XRD analyses, which would be inapplicable due to its detection limit. For the sample of oxd-Ni/CNHs, a single peak would reflect a combination of reduction of NiO and gasification of carbon content. Finally, there was only a single peak when the sample of red-oxd-Ni/CNHs was subject to the temperature above 500 °C, suggesting the presence of metallic Ni within the sample. As shown in the supporting material (S.02), FT-IR spectra confirmed that there were similar functional groups on the surface of all Ni/CNH samples though they were treated with different conditions.

3.2 Catalytic performance

Performance of each catalyst was separately tested in the so-called catalytic transfer hydrogenation of ML to produce GVL by supplying 2-propanol as H-donor instead of using H2 gas. The schematic representation of ML-to-GVL conversion was shown in Fig. 5. Based on GC analyses of the resultant liquid product, the performance of each catalyst was summarized in Table 2. Without and with pristine CNHs incorporation, conversion of ML and yield of GVL was rather low and in the same order of magnitude. As Ni species was impregnated onto CHNs, conversion of ML (9.5%) and selectivity of GVL formation (84.1%) were detectably higher than that of CNHs alone. Reduction of Ni/CNHs could result in a further increase in conversion of ML (38.7%) and selectivity of GVL (98.7%), resulted from the influence of higher catalytic activity of Ni species after the reduction process. However, oxidation of Ni/CNHs would result in the formation of oxide of Ni species existing in oxd-Ni/CNHs, leading to lower conversion of ML (12.8%) and selectivity of GVL (68.5%). Interestingly, red-oxd-Ni/CNHs could exhibit the best catalytic performance with regard to the highest conversion of ML (96.2%) and selectivity of GVL (93.0%). It should be noted that Ni/AC could provide moderate catalytic activity, which could result in the 71.1% conversion of ML and 57.7% selectivity of GVL. Ni/CNTs give similar ML conversion of 98.6% but clearly lower selectivity of GVL (82.1%) as compared with the red-oxd-Ni/CNHs. The result would be ascribed that some of Ni nanoparticles on the outer surface of CNTs were directly accessible but most of them were agglomerated as showed Fig. 2(e). On the contrary, most of Ni nanoparticles were embedded within the porous structure of CNHs so that less amount of ML could directly contact with Ni nanoparticles within Ni/CNHs, resulted in lower conversion. However, such higher yield and selectivity of GVL would be resulted from the lower agglomeration of Ni nanoparticles when compared to those in Ni/CNTs. In addition, it is considered that the pore confinement in CNHs may help improve the GVL selectivity as the Ni particle in the horn channel could selectively accommodate a cyclization reaction to form GVL [10]. Furthermore, confirmation of difference in catalytic performance of NiO and metallic Ni

species summarized in Table 2 would suggest that incorporation of Ni nanoparticles onto carbonaceous support materials would provide synergetic effects on catalytic performance of Ni hybridized with CNHs. Such hybridization of Ni nanoparticles embedded in porous structure of CNHs could play a significant role in the transfer hydrogenation of ML to produce GVL.

The effect of reaction temperature on the catalytic performance of red-oxd-Ni/CNHs was shown in Fig. 6. The red-oxd-Ni/CNH catalyst showed extremely low activity (ML conversion below 10%) at the reaction temperature of 140 and 170 °C while the ML conversion was enhanced up to 90% at 200 °C. In addition, the high GVL selectivity suggested that the red-oxd-Ni/CNH catalyst could result in a few side-reactions. All results based on the increase in the reaction temperature from 140 to 200 °C, which could significantly enhance the ML conversion as well as the GVL yield and selectivity, align with an endothermic nature of the transfer hydrogenation of ML to form GVL [20].

More interestingly, Fig. 7 presented the catalytic reusability of red-oxd-Ni/CNH catalyst after it was employed for converting ML over 5 repeated cycles. Only a slight decline in the conversion of ML was detected while the selectivity of GVL was still higher than 85% even after five cycles, indicating that the red-oxd-Ni/CNHs could exhibit high stability and reusability for GVL production. These results would be ascribed that the hybridization of Ni nanoparticles within the stable structure of CNHs could help prevent the agglomeration of Ni nanoparticles therefore they could maintain their good catalytic performance.

4. Conclusions

Facile synthesis of the novel catalyst of Ni hybridized with CNHs (Ni/CNHs) could be achieved by the one-step GI-AIW method. Strategic manipulation using oxidation and reduction of Ni/CNHs could lead to significant difference in the BET surface area and Ni nanoparticle dispersion within the resultant Ni/CNHs, which consequently affect their catalytic performance in the transfer hydrogenation of ML to produce GVL. With red-oxd-Ni/CNHs, 96.2% conversion of ML with 93% selectivity of GVL could be achieved by using 2-propanol as H-donor instead of H2. Only an insignificant decline in catalytic performance of the red-oxd-Ni/CNHs was observed though they were employed in five runs of the ML transfer hydrogenation because of the less agglomeration of Ni nanoparticles. As a unique finding result, with CNHs as the support material, Ni could exert a better catalytic activity than the unsupported Ni and the Ni supported on activated carbon and CNTs.
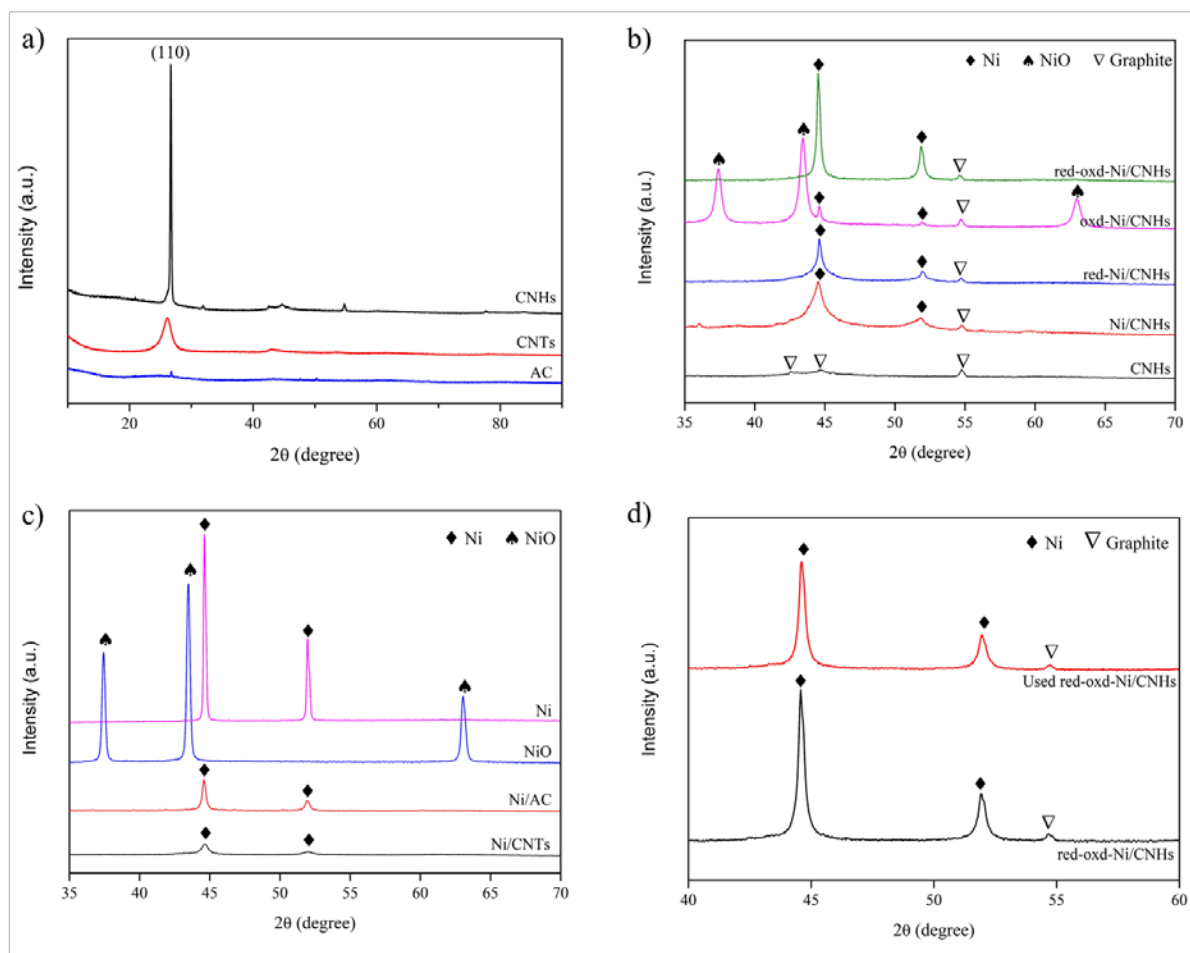
Fig. 1 XRD patterns of (a) carbonaceous support materials, (b) Ni/CNHs catalysts treated with different thermal conditions, (c) Ni catalysts under different conditions, and (d) fresh and used red-oxd-Ni/CNHs catalysts
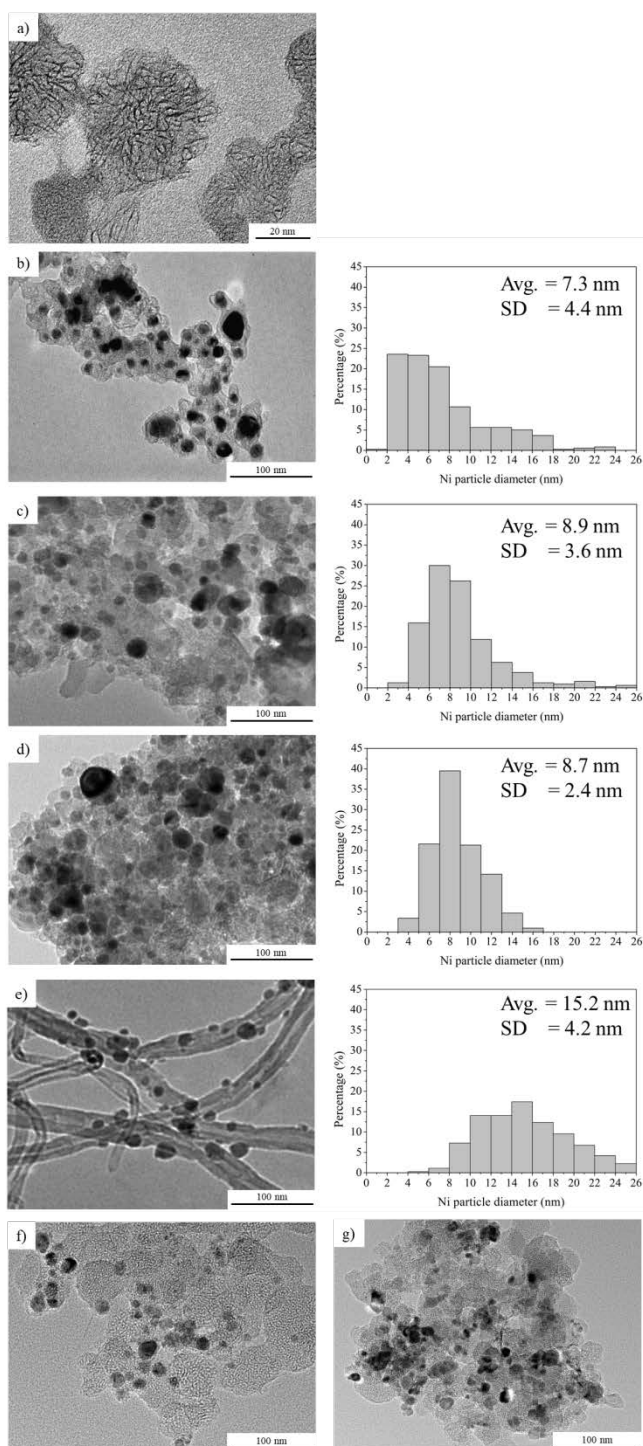
Fig. 2 TEM images and particle size distributions of (a) CNHs, (b) Ni/CNHs, (c) red-oxd-Ni/CNHs, (d) used red-oxd-Ni/CNHs, (e) Ni/CNTs, (f) red-Ni/CNHs, and (g) oxd-Ni/CNHs

Annual Activity Report on Japan-ASEAN Science, Technology and Innovation Platform (JASTIP),
Work Package 2 (WP2) - Energy and Environment

P a g e 37 | 48
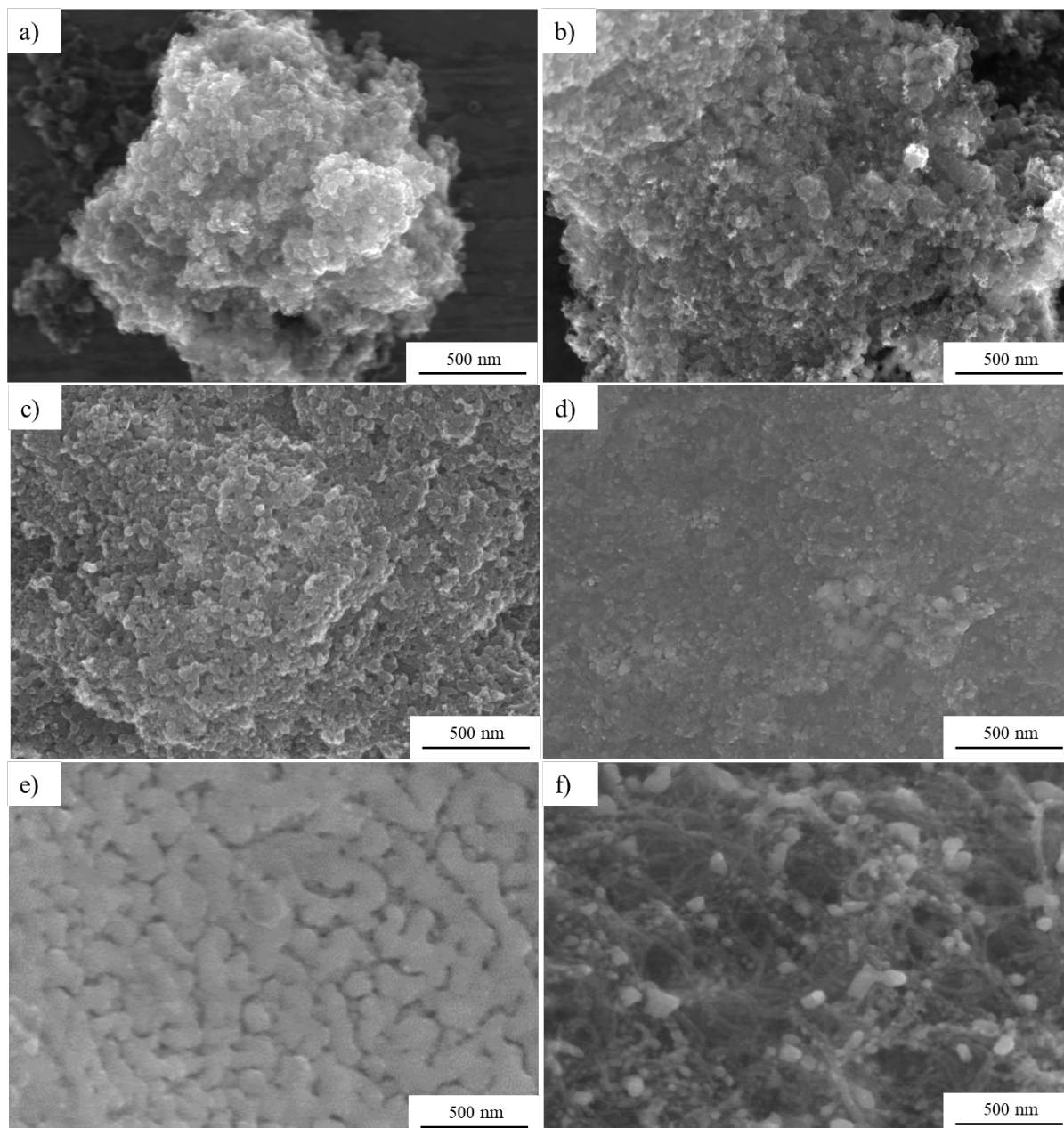
Fig. 3 FE-SEM images of (a) red-Ni/CNHs, (b) oxd-Ni/CNHs, (c) red-oxd-Ni/CNHs, (d) used red-oxd-Ni/CNHs, (e) Ni/AC, and (f) Ni/CNTs

Annual Activity Report on Japan-ASEAN Science, Technology and Innovation Platform (JASTIP),
Work Package 2 (WP2) - Energy and Environment

P a g e 38 | 48

Fig. 4 H$_2$-TPR profiles of Ni/CNHs treated with different thermal conditions

Fig. 5 Schematic representation of ML-to-GVL conversion.

Annual Activity Report on Japan-ASEAN Science, Technology and Innovation Platform (JASTIP),
Work Package 2 (WP2) - Energy and Environment

P a g e 39 | 48

Fig. 6 Effect of reaction temperature for ML-to-GVL conversion (reaction time of 3 h, catalyst loading of 0.1 g)
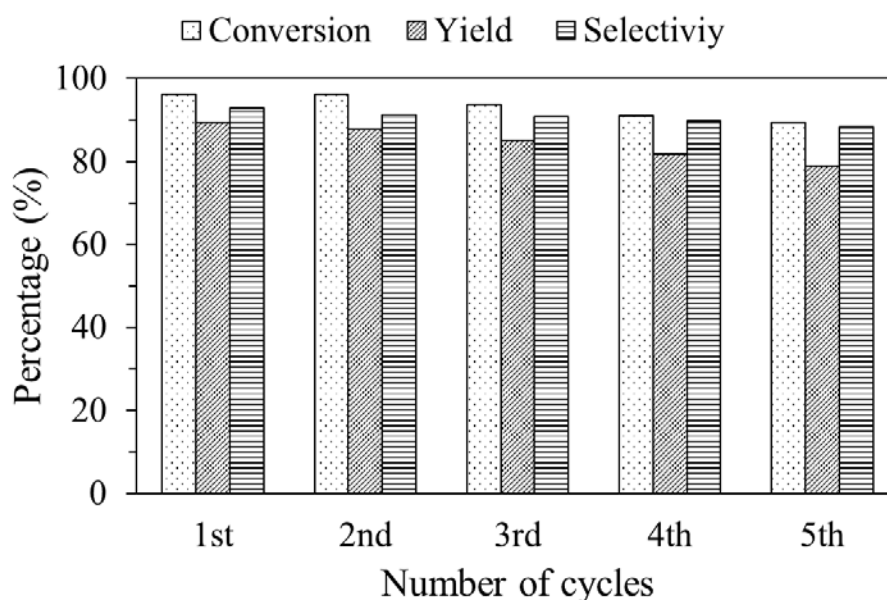
Fig. 7 Reusability of red-oxd-Ni/CNHs for ML-to-GVL conversion. Reaction conditions: reaction temperature of 200 °C, reaction time of 3 h, catalyst loading of 0.1 g

Annual Activity Report on Japan-ASEAN Science, Technology and Innovation Platform (JASTIP),
Work Package 2 (WP2) - Energy and Environment

P a g e 40 | 48

Table 1 BET surface area and Ni content of each catalyst sample

Catalysts	BET surface area [m²/g]	Ni content [wt%]
CNHs	162.4	0[S,E,T]
Ni/CNHs	134.5	15[E],21[T]
red-Ni/CNHs	236.9	17[E],25[T]
oxd-Ni/CNHs	225.1	20[E],33[T]
red-oxd-Ni/CNHs	250.5	22[E],36[T]
AC	1062.7	0[S,E]
Ni/AC	373.3	20[S],28[E]
CNTs	118.9	0[S,E]
Ni/CNTs	135.5	20[S],15[E]
NiO	2.5	79[S],80[E]
Ni	0.7	100[S,E]

Superscript S means Ni content stoichiometrically calculated from precursors with assumption that carbon is not lost during the Ni-loading process. Superscripts E and T at Ni content values stand for values evaluated by SEM-EDX surface-based analysis and TGA, respectively.

Table 2 Catalytic performance of each catalyst sample in ML-to-GVL conversion

Catalysts	%Conversion	%Yield	%Selectivity
w/o catalyst	6.5	3.3	51.4
CNHs	4.7	2.9	61.4
Ni/CNHs	9.5	8.0	84.1
red-Ni/CNHs	38.7	38.2	98.7
oxd-Ni/CNHs	12.8	8.7	68.5
red-oxd-Ni/CNHs	96.2	89.4	93.0
Ni/AC	71.1	41.0	57.7
Ni/CNTs	98.6	81.0	82.1
NiO	3.8	3.1	82.1
Ni	65.7	45.3	69.0

Reaction conditions: T = 200 °C, Time = 3 h, Catalyst loading = 0.1 g.

Annual Activity Report on Japan-ASEAN Science, Technology and Innovation Platform (JASTIP), Work Package 2 (WP2) - Energy and Environment

P a g e 41 | 48

References

[1] Z. Rong, Z. Sun, L. Wang, J. Lv, Y. Wang, Y. Wang, Efficient Conversion of Levulinic Acid into γ-Valerolactone over Raney Ni Catalyst Prepared from Melt-quenching Alloy, Catal. Lett., 144 (2014) 1766-1771.

[2] A.M. Hengne, B.S. Kadu, N.S. Biradar, R.C. Chikate, C.V. Rode, Transfer hydrogenation of biomass-derived levulinic acid to [gamma]-valerolactone over supported Ni catalysts, RSC Adv., 6 (2016) 59753-59761.

[3] B. Cai, X.-C. Zhou, Y.-C. Miao, J.-Y. Luo, H. Pan, Y.-B. Huang, Enhanced Catalytic Transfer Hydrogenation of Ethyl Levulinate to γ-Valerolactone over a Robust Cu–Ni Bimetallic Catalyst, ACS Sustainable Chem. Eng., 5 (2017) 1322-1331.

[4] L. Negahdar, M.G. Al-Shaal, F.J. Holzhäuser, R. Palkovits, Kinetic analysis of the catalytic hydrogenation of alkyl levulinates to γ-valerolactone, Chem. Eng. Sci., 158 (2017) 545-551.

[5] X. Tang, X. Zeng, Z. Li, L. Hu, Y. Sun, S. Liu, T. Lei, L. Lin, Production of γ-valerolactone from lignocellulosic biomass for sustainable fuels and chemicals supply, Renewable Sustainable Energy Rev., 40 (2014) 608-620.

[6] X. Tang, Z. Li, X. Zeng, Y. Jiang, S. Liu, T. Lei, Y. Sun, L. Lin, In Situ Catalytic Hydrogenation of Biomass-Derived Methyl Levulinate to gamma-Valerolactone in Methanol, ChemSusChem, 8 (2015) 1601-1607.

[7] Z. Xue, J. Jiang, G. Li, W. Zhao, J. Wang, T. Mu, Zirconium-cyanuric acid coordination polymer: highly efficient catalyst for conversion of levulinic acid to [gamma]-valerolactone, Catal. Sci. Technol., 6 (2016) 5374-5379.

[8] A.H. Valekar, K.-H. Cho, S.K. Chitale, D.-Y. Hong, G.-Y. Cha, U.H. Lee, D.W. Hwang, C. Serre, J.-S. Chang, Y.K. Hwang, Catalytic transfer hydrogenation of ethyl levulinate to [gamma]-valerolactone over zirconium-based metal-organic frameworks, Green Chem., 18 (2016) 4542-4552.

[9] Z.P. Yan, L. Lin, S. Liu, Synthesis of γ-Valerolactone by Hydrogenation of Biomass-derived Levulinic Acid over Ru/C Catalyst, Energy Fuels, 23 (2009) 3853-3858.

[10] A.S. Piskun, J.E. de Haan, E. Wilbers, H.H. van de Bovenkamp, Z. Tang, H.J. Heeres, Hydrogenation of Levulinic Acid to γ-Valerolactone in Water Using Millimeter Sized Supported Ru Catalysts in a Packed Bed Reactor, ACS Sustainable Chem. Eng., 4 (2016) 2939-2950.

[11] L.E. Manzer, Catalytic synthesis of α-methylene-γ-valerolactone: a biomass-derived acrylic monomer, Appl. Catal., A, 272 (2004) 249-256.

[12] A.A. Smirnov, S.A. Khromova, O.A. Bulavchenko, V.V. Kaichev, A.A. Saraev, S.I. Reshetnikov, M.V. Bykova, L.I. Trusov, V.A. Yakovlev, Effect of the Ni/Cu ratio on the composition and catalytic properties of nickel-copper alloy in anisole hydrodeoxygenation, Kinet. Catal., 55 (2014) 69-78.

[13] K. Murata, K. Kaneko, W.A. Steele, F. Kokai, K. Takahashi, D. Kasuya, K. Hirahara, M. Yudasaka, S. Iijima, Molecular potential structures of heat-treated single-wall carbon nanohorn assemblies, The Journal of Physical Chemistry B, 105 (2001) 10210-10216.

[14] N. Sano, K. Taniguchi, H. Tamon, Gas flow rate in the gas-injected arc-in-water method as a critical factor to synthesize high-dispersion Pd-Ni alloy nanoparticles in single-walled carbon nanohorns, Journal of Chemical Engineering of Japan, 47 (2014) 821-826.

[15] N. Sano, Y. Kimura, T. Suzuki, Synthesis of Carbon Nanohorns by a Gas-Injected Arc-in-Water Method and Application to Catalyst-Support for Polymer Electrolyte Fuel Cell Electrodes, J. Mater. Chem., 18 (2008) 1555.

[16] S. Zhu, G. Xu, Single-Walled Carbon Nanohorns and Their Applications, Nanoscale, 2 (2010) 2538-2549.

[17] L. Sun, C. Wang, Y. Zhou, X. Zhang, B. Cai, J. Qiu, Flowing nitrogen assisted-arc discharge synthesis of nitrogen-doped single-walled carbon nanohorns, Applied Surface Science, 277 (2013) 88-93.

[18] C. Poonjarernsilp, N. Sano, T. Charinpanitkul, H. Mori, T. Kikuchi, H. Tamon, Single-Step Synthesis and Characterization of Single-Walled Carbon Nanohorns Hybridized with Pd Nanoparticles Using N2 Gas-Injected Arc-In-Water Method, Carbon, 49 (2011) 4920-4927.

[19] C. Dong, A.S. Campell, R. Eldawud, G. Perhinschi, Y. Rojanasakul, C.Z. Dinu, Effects of acid treatment on structure, properties and biocompatibility of carbon nanotubes, Applied Surface Science, 264 (2013) 261-268.

[20] E. Lam, J.H.T. Luong, Carbon Materials as Catalyst Supports and Catalysts in the Transformation of Biomass to Fuels and Chemicals, ACS Catal., 4 (2014) 3393-3410.

[21] S. Gómez, N.M. Rendtorff, E.F. Aglietti, Y. Sakka, G. Suárez, Surface modification of multiwall carbon nanotubes by sulfonitric treatment, Applied Surface Science, 379 (2016) 264-269.

[22] C. Poonjarernsilp, N. Sano, H. Tamon, Hydrothermally Sulfonated Single-Walled Carbon Nanohorns for Use as Solid Catalysts in Biodiesel Production by Esterification of Palmitic Acid, Appl. Catal. B, 147 (2014) 726-732.

[23] L.C.A. Oliveira, C.N. Silva, M.I. Yoshida, R.M. Lago, The effect of H2 treatment on the activity of activated carbon for the oxidation of organic contaminants in water and the H2O2 decomposition, Carbon, 42 (2004) 2279-2284.

[24] N. Sano, T. Suntornlohanakul, C. Poonjarernsilp, H. Tamon, T. Charinpanitkul, Controlled syntheses of various palladium alloy nanoparticles dispersed in single-walled carbon nanohorns by one-step formation using an arc discharge method, Industrial & Engineering Chemistry Research, 53 (2014) 4732-4738.

[25] A.B. Dongil, B. Bachiller-Baeza, I. Rodriguez-Ramos, J.L.G. Fierro, N. Escalona, The effect of Cu loading on Ni/carbon nanotubes catalysts for hydrodeoxygenation of guaiacol, RSC Adv., 6 (2016) 26658-26667.

[26] N. Sano, D. Himara, H. Tamon, Simultaneous enhancement in porosity and magnetic property of Fe-dispersing single-walled carbon nanohorns by oxidation using CO2, Chemical Engineering Journal, 271 (2015) 43-49.

[27] Y. Xing, L. Li, C.C. Chusuei, R.V. Hull, Sonochemical Oxidation of Multiwalled Carbon Nanotubes, Langmuir, 21 (2005) 4185-4190.

[28] J. Zhang, C. Chen, W. Yan, F. Duan, B. Zhang, Z. Gao, Y. Qin, Ni nanoparticles supported on CNTs with excellent activity produced by atomic layer deposition for hydrogen generation from the hydrolysis of ammonia borane, Catal. Sci. Technol., 6 (2016) 2112-2119.

[29] J. Wang, D. Teschner, Y. Yao, X. Huang, M. Willinger, L. Shao, R. Schlogl, Fabrication of nanoscale NiO/Ni heterostructures as electrocatalysts for efficient methanol oxidation, J. Mater. Chem. A, 5 (2017) 9946-9951.

Annual Activity Report on Japan-ASEAN Science, Technology and Innovation Platform (JASTIP), Work Package 2 (WP2) - Energy and Environment

P a g e 43 | 48

3.2.2 *Development of ultra-fast method to prepare activated carbon using microwave irradiation into KOH activation*

Microwave-irradiation function can be installed in the activating reactor system to realize fast and uniform heating in KOH activation to prepare activated carbon. It has been reported that a condition under microwave irradiation can reduce the heating time. If the condition of the microwave irradiation is appropriately tuned, the heating time in the activation step will be highly reduced. Fig. 6 shows the photograph of the hand-made microwave-irradiation reactor to realize fast activation step, used in my experiment.

It was aimed to develop a new method to realize the fast preparation of activated carbon with large specific surface area above 1000 m^2/g, and it was wanted to investigate the applications of the high-surface-area products. The methods used for these objectives are (1) addition of microwave-irradiation function in the KOH activation process, and (2) investigation of the applications for electric double layer capacitor (EDLC).

The most significant novel point in the results is the use of the microwave-irradiation in the KOH activation, and the discovery of the appropriate condition based on this method leads to the extremely fast synthesis of the activated carbon which has the surface area above 1000 m2/g.
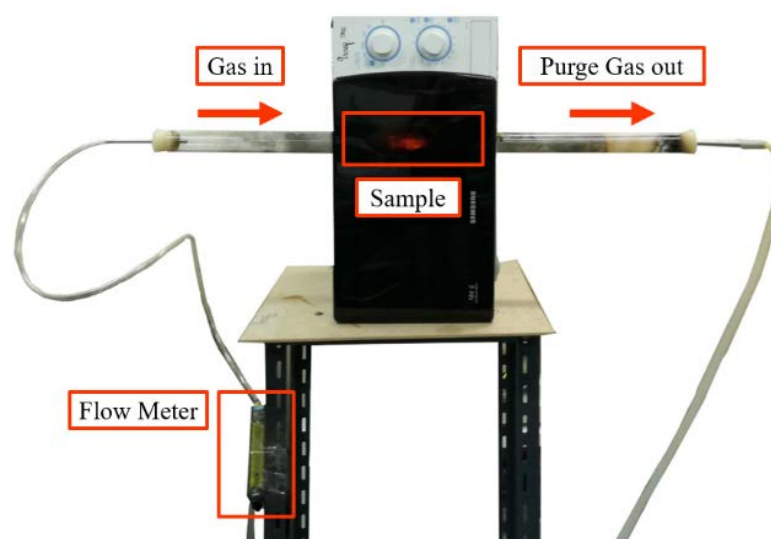
Fig. 8 Microwave irradiation system

Annual Activity Report on Japan-ASEAN Science, Technology and Innovation Platform (JASTIP),
Work Package 2 (WP2) - Energy and Environment

P a g e 44 | 48

3.2.3 Development of Fe-dispersed carbon nanohorns for H_2 storage–carbon nanohorns dispersed with Fe nanoparticles have been developed, and its H_2 storage mechanism has been investigated by molecular orbital calculation

Using gas-injected arc-in-water method developed by our group, pure-carbon single-walled carbon nanohorns (p-SWCNHs), Fe-dispersed carbon nanohorns (SWCNHs/Fe) and SWCNHs/Fe on which pores are opened by oxidation-reduction treatment (ox-SWCNHs) were synthesized. It was found that the dispersion of Fe in SWCNHs lead to higher H_2 storage amount. It was considered that this increase of H_2 storage amount could be caused by so-called H_2 spillover effect. To clarify this effect theoretically, semi-empirical molecular orbital calculation was carried out on modeled structure of SWCNH into which a Fe cluster is put with relaxed structure. Fig. 9 (A) shows the modeled structure, and Fig. 9(B) shows the energy change of this structure with varied inter H-H distance with different H_2-SWCNH gas D. The decrease of the value of ΔE in this figure means that the H_2 spillover effect can more preferably take place. As a result, when H_2 molecule is placed in closer position to SWCNHs, the decrease of ΔE can become more prominent. This result may indicate that the higher the pressure of H_2, the larger the H_2 storage amount due to the H_2 spillover effect.
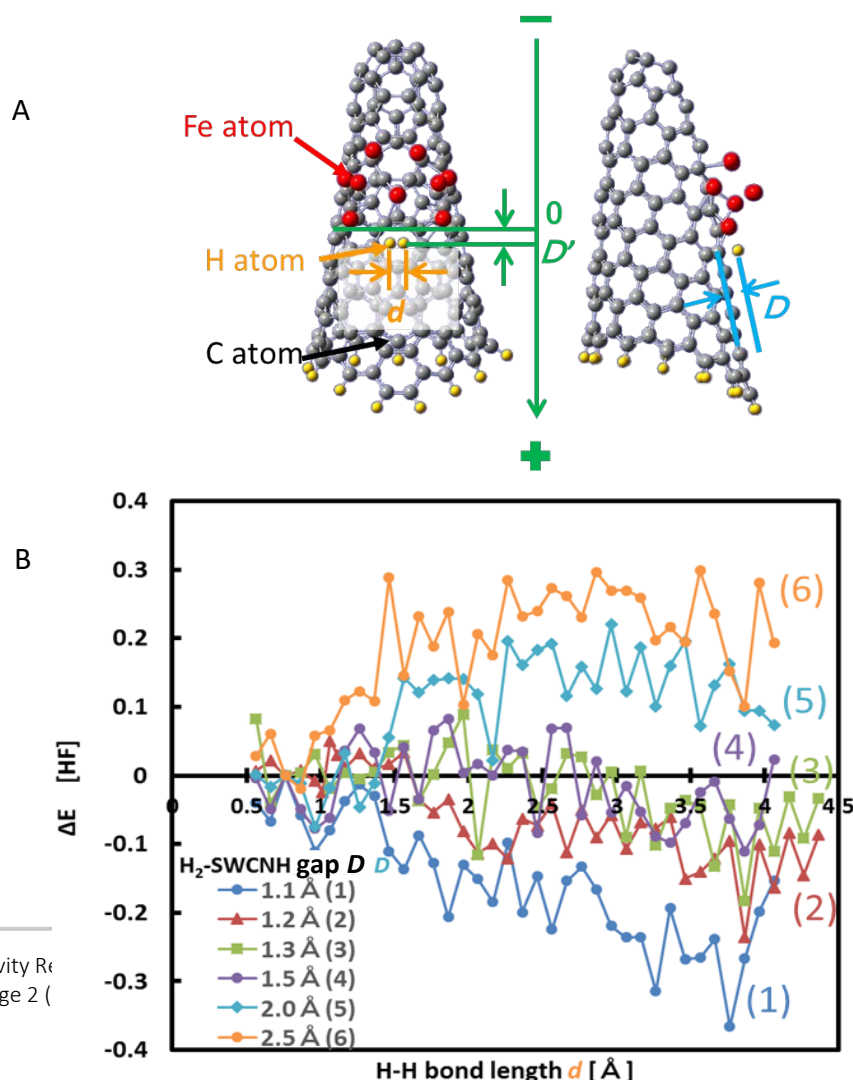
Fig. 9 (A) Model of SWCHNs for molecular orbital calculation with varied position of H_2 molecule and degree of H_2 dissociation. (B) Total energy of H_2-adsorbed structures with varied inter H-H distance with different $_{H2}$-SWCNH gas D.

3.3 Outputs

1.3.1 Publication

- K. Kerdnawee, P. Kuptajit, N. Sano, H. Tamon, W. Chaiwat, T. Charinpanitkul, Catalytic Ozonation of Oxy-tetracycline Using Magnetic Carbon Nanoparticles, Journal of the Japan Institute of Energy, 96 (2017)362-366.

-C. Termvidchakorn, N. Sano, H. Tamon, N. Viriya-Empikul, K. Faungnawakij, T. Charinpanitkul Conversion of D-Xylose to Furfural via Catalytic Dehydration Using Carbon Nanohorns Hybridized with NiCu Nanoparticles, Journal of the Japan Institute of Energy, 96 (2017) 380-385.

- C. Termvidchakorn, V. Itthibenchapong, S. Songtawee, B. Chamnankid, S. Namuangruk, K. Faungnawakij, T. Charinpanitkul, R. Khunchit, N. Hansupaluk, N. Sano and H. Hinode, Dehydration of D-xylose to furfural using acid-functionalized MWCNTs catalysts, Adv. Nat. Sci.: Nanosci. Nanotechnol. 8, (2017) 035006.

- C. Termvidchakorn, K. Faungnawakij*, S. Kuboon, T. Butburee, N. Sano, T. Charinpanitkul*, A novel catalyst of Ni hybridized with single-walled carbon nanohorns for converting methyl levulinate to γ-valerolactone, Applied Surface Science, In press 2018

1.3.2 Conference and Forum

- Chompoopitch Termvidchakorn, Kajornsak Faungnawakij, Noriaki Sano, and Tawatchai Charinpanitkul*, The Effect of Treatment Duration on Sulfonated Single-Walled Carbon Nanohorns, The 6th joint conference on renewable energy and nanotechnology (JCREN2017), 12-14 October 2017, Bangkok, Thailand

- Noriaki Sano*, Shoichi Tsunauchi, Tatporn Suntornlohanakul, Chompoopitch Termvidchakorn, Chuleeporn Luadthong, Kajornsak Faugnawakij, and Tawatchai Charinpanitkul, Features in Metal-Dispersed Single-Walled Carbon Nanohorns Prepared Using Gas-Injected Arc-in-Water Method for Catalyst Applications, The 6th joint conference on renewable energy and nanotechnology (JCREN2017), 12-14 October 2017, Bangkok, Thailand

- Konrat Kerdnawee, Noriaki Sano and Tawatchai Charinpanitkul*, Adsorption of oxy-tetracycline antibiotic on magnetic carbon nanoparticles, The 6th joint conference on renewable energy and nanotechnology (JCREN2017), 12-14 October 2017, Bangkok, Thailand

- Kajornsak Faungnawakij, NANOTEC R&D activities on Heterogeneous Nanocatalysts for Biorefinery Applications, The 6th joint conference on renewable energy and nanotechnology (JCREN2017), 12-14 October 2017, Bangkok, Thailand

- Kajornsak Faungnawakij*, Nanocatalyst Applications in a Biorefinery Scheme, The First Materials Research Society of Thailand International Conference (1st MRS Thailand International Conference), October 31 – November 3, 2017, The Empress Convention Center, Chiang Mai, Thailand

- Kajornsak Faungnawakij*, Chuleeporn Luadthong, Pongtanawat Khemthong, Copper ferrite spinel oxide catalysts for methanolysis of palm oil, the 25th European Biomass Conference & Exhibition (EUBCE 2017), 12-15 June 2017, Stockholm, Sweden

- Kajornsak Faungnawakij, Development and Applications of Nanocatalysts in a Biorefinery Scheme, 10th Kyoto University Southeast Asia Network Forum and 28th Kyoto University Southeast Asia Forum, 24 February 2018, Bangkok, Thailand

- Kajornsak Faungnawakij, Nanocatalysts for Biofuels and Biochemicals, Pure and Applied Chemistry International Conference (PACCON 2018), 7-9 February 2018, Hat yai, Thailand

1.3.3 Book

- Vorranutch Itthibenchapong, Atthapon Srifa, Kajornsak Faungnawakij, "Ch.11 Heterogeneous Catalysts for Advanced Biofuel Production" in "Nanotechnology for Bioenergy and Biofuel Production" Editors Mahendra Rai and Silvio Silverio da Silva, Springer 2017.

1.3.4 Award

- Best Poster Presentation: K. Kerdnawee, N. Sano, T. Charinpanitkul, Adsorption of oxy-tetracycline antibiotic on magnetic carbon nanoparticles, The 6th Joint Conference on Renewable Energy and Nanotechnology (JCREN2017)

- Best Oral Presentation: P. Kuptajit, T. Kamolvatanavit, N. Sano, T. Charinpanitkul, Activated carbon powders derived from water hyacinth. The 6th joint conference on renewable energy and nanotechnology (JCREN2017)

- CST Citation Award 2017: Kajornsak Faungnawakij

- TRF-OHEC-SCOPUS Researcher Award 2017: Kajornsak Faungnawakij

1.3.5 Student exchange

- Two students from Chulalongkorn University visited Kyoto Univ. for research exchange program under JASTIP, June 2017.
    - Ms. PURICHAYA KUPTAJIT   Master student, Chulalongkorn University
    - Ms. KARANICK MINAKANISHTHA Master student, Chulalongkorn University

- Two JASTIP seminars of the project were held in 2017 at NANOTEC (Sep, 26: Five Japanese members visited NANOTEC and Chulalongkorn Univ and at Kyoto univ (Nov, 16: Four Thai members visited Kyoto Univ.).
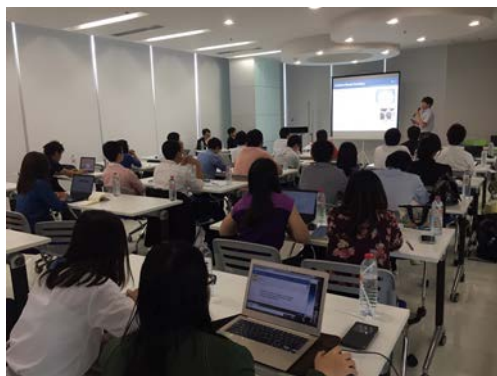
Fig. 10 Seminars and lab visits in Thailand and Japan during 2017FY.

Annual Activity Report on Japan-ASEAN Science, Technology and Innovation Platform (JASTIP), Work Package 2 (WP2) - Energy and Environment

P a g e 48 | 48